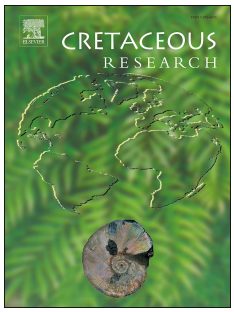

The Uppermost Cretaceous Continental Deposits at the Southern end of Patagonia, the Chorrillo Formation case study (Austral-Magallanes Basin): Sedimentology, fossil content and regional implications

D. Moyano-Paz, S. Rozadilla, F. Agnolín, E. Vera, M.D. Coronel, A.N. Varela, A.R. Gómez-Dacal, A.M. Aranciaga-Rolando, J. D'Angelo, V. Pérez-Loinaze, S. Richiano, N. Chimento, M.J. Motta, J. Sterli, M. Manabe, T. Tsuihiji, M.P. Isasi, D.G. Poiré, F.E. Novas

PII: S0195-6671(21)00307-4

DOI: https://doi.org/10.1016/j.cretres.2021.105059

Reference: YCRES 105059

To appear in: *Cretaceous Research*

Received Date: 13 May 2021

Revised Date: 16 September 2021

Accepted Date: 1 October 2021

Please cite this article as: Moyano-Paz, D., Rozadilla, S., Agnolín, F., Vera, E., Coronel, M.D., Varela, A.N., Gómez-Dacal, A.R., Aranciaga-Rolando, A.M., D'Angelo, J., Pérez-Loinaze, V., Richiano, S., Chimento, N., Motta, M.J., Sterli, J., Manabe, M., Tsuihiji, T., Isasi, M.P., Poiré, D.G., Novas, F.E., The Uppermost Cretaceous Continental Deposits at the Southern end of Patagonia, the Chorrillo Formation case study (Austral-Magallanes Basin): Sedimentology, fossil content and regional implications, *Cretaceous Research*, https://doi.org/10.1016/j.cretres.2021.105059.

Authors contribution

Moyano-Paz: Conceptualization, Fieldwork, Investigation, Writing – Original Draft, Figure Editing, Project Leader.

Rozadilla: Fieldwork, Investigation, Writing – Original Draft, Figure Editing, Material analysis.

Agnolin: Fieldwork, Investigation, Writing – Original Draft, Figure Editing, Material analysis

Vera: Fieldwork, Investigation, Writing – Original Draft, Figure Editing, Material analysis

Coronel: Fieldwork, Investigation, Writing – Original Draft, Figure Editing

Varela: Investigation, Writing – Original Draft, Figure Editing

Gómez-Dacal: Investigation, Writing – Original Draft, Figure Editing

Aranciaga-Rolando: Fieldwork, Writing – Original Draft, Material analysis

D'Angelo: Fieldwork, Writing – Original Draft, Material analysis

Perez-Loinaze: Investigation, Writing – Original Draft, Figure Editing

Richiano: Investigation, Writing – Original Draft, Figure Editing

Chimento: Fieldwork, Investigation, Material analysis

Motta: Fieldwork, Investigation, Material analysis

Sterli: Investigation, Writing – Original Draft, Material analysis

Manabe: Fieldwork, Investigation, Writing – Original Draft, Figure Editing

Tsuihiji: Fieldwork, Investigation, Writing – Original Draft, Figure Editing

Isasi: Fieldwork, Investigation, administration

Poiré: administration, Founding acquisition, Review original draft

Novas: Fieldwork, Investigation, Review – original draft, Founding acquisition, Project leader

The Uppermost Cretaceous Continental Deposits at the Southern end of Patagonia, the Chorrillo Formation case study (Austral-Magallanes Basin): Sedimentology, fossil content and regional implications

Moyano-Paz, D[1]., Rozadilla, S[2]., Agnolín, F[2,3]., Vera, E[4,5]., Coronel, M.D[1]., Varela, A.N[6]., Gómez-Dacal, A.R[6]., Aranciaga-Rolando, A.M[2]., D`Angelo, J.S[2]., Pérez-Loinaze, V[4]., Richiano, S., Chimento, N.R[2]., Motta, M.J[2]., Sterli, J[8]., Manabe, M[9]., Tsuihiji, T[10]., Isasi, M.P[2]., Poiré, D.G[1]., Novas, F.E[2].

[1] *Centro de Investigaciones Geológicas (CONICET – UNLP), Diagonal 113 275, B1904DPK, La Plata, Buenos Aires, Argentina.*

[2] *Laboratorio de Anatomía Comparada y Evolución de los Vertebrados del Museo Argentino de Ciencias Naturales "Bernardino Rivadavia" (CONICET), Av. Ángel Gallardo 470, C1405DJR, Ciudad Autónoma de Buenos Aires, Argentina.*

[3] *Fundación de Historia Natural "Félix de Azara", Departamento de Ciencias Naturales y Antropología. CEBBAD - Universidad Maimónides. Hidalgo (C1405BDB), Buenos Aires, Argentina*

[4] *División Paleobotánica. Museo Argentino de Ciencias Naturales "Bernardino Rivadavia", CONICET, Av. Ángel Gallardo 470, C1405DJR, Buenos Aires, Argentina*

[5] *Área de Paleontología, Departamento de Geología, Universidad de Buenos Aires, Pabellón 2, Ciudad Universitaria, C1428EGA, Buenos Aires, Argentina*

[6] *Y-TEC (YPF S.A. – CONICET), Av. Del Petróleo s/n entre 129 y 143, Berisso, Buenos Aires, Argentina.*

[7] *Instituto Patagónico de Geología y Paleontología (CONICET – CENPAT), Boulevard Brown 2915, U9120ACD Puerto Madryn, Argentina*

[8] *CONICET-Museo Paleontológico Egidio Feruglio, Av. Fontana 140, 9100 Trelew, Argentina*

[9] *Center for the Collections, National Museum of Nature & Science, Tsukuba 305-0005, Japan.*

[10] *Department of Geology & Paleontology, National Museum of Nature & Science, Tsukuba 305-0005, Japan.*

Abstract. The deposits of the Chorrillo Formation (Maastrichtian) were accumulated during a 'continental window' that occurred during the Late Cretaceous in the Austral-Magallanes foreland basin, southern Patagonia, Argentina. The aim of the present contribution is to describe the depositional conditions as well as new vertebrate and plant fossils from this unit. The analysis of these deposits resulted in the definition of five architectural elements: Complex sandy narrow sheets channels (SS), Complex gravelly narrow sheets channels (GS), Sandstone lobes (SL), Thick fine-grained deposits (GF) and Thin dark fine-grained deposits (DF). These were separated into channelized and non-channelized units and represent the accumulation in a fine-grained dominated, fossil rich fluvial depositional system. Vertebrates fossil records include two species of frogs of the genus *Calypteocephalella* (representing the southernmost record of Pipoidea), snakes belonging to Madtsoiidae and Anilioidea (the latter ones being the first records for the basin), chelid turtles similar to *Yaminuechelys-Hydromedusa*, meiolaniiform turtles, titanosaur sauropods, megaraptoran theropods, new remains of the elasmarian *Isasicursor santacrucensis* (including the first cranial remains available for this species), hadrosaur ornithischians, enantiornithine birds. Sharks and elasmosaurs are also recorded and may possibly derive from the overlying marine Calafate Formation. These new taxa, together with previous findings from the Chorrillo Formation, are included into a stratigraphic column, thus providing valuable information that sheds new light on faunistic composition and paleobiogeography of high-latitude biotas of Gondwana.

Keywords: foreland basin, fluvial system, paleobotany, fossil vertebrates, continentalization, Maastrichtian.

1. INTRODUCTION

The onset of the retroarc foreland phase of the Austral-Magallanes Basin caused an important flexural deeping of the foredeep depocenter (Natland et al., 1974) and is characterized by a thick deep-marine sedimentation that took place during the early Late Cretaceous (~101 Ma; Fildani and Hessler, 2005; Romans et al., 2009; Fosdick et al., 2011; Malkowski et al., 2015, 2017; Daniels et al., 2018). The migration of the shoreline toward the southeast resulted in the installation of deltaic shorelines that marked the end of the deep-marine accumulation during the Santonian-Campanian (Moyano-Paz et al., 2018, 2020; Ghiglione et al., 2021). This progressive advance towards the southeast of the coastline triggered a complete continentalization of the foredeep main depocenter of the basin (Fig. 1a; Cuitiño et al., 2019; Varela et al., 2019), in the Lago Argentino region, from the Campanian to the Maastrichtian (Sickmann et al., 2018; Tettamanti et al., 2018; Cuitiño et al., 2019; Ghiglione et al., 2021).

The Maastrichtian Chorrillo Formation is the youngest of the units that accumulated during the period of complete continentalization of the basin at this latitude. This unit has been the focus of paleontological studies since the 1940s (Feruglio, 1945; Bonaparte, 1996; Bonaparte et al., 2002), but its paleontological content was not analyzed in some detail until recent years (Novas et al., 2019; Chimento et al., 2020, 2021; Rozadilla et al., 2021). Moreover, in spite of the paleontological importance of the Chorrillo Formation, there have been no detailed sedimentological studies that would provide insights into the depositional conditions under which it was accumulated.

The first fossil vertebrates from the Chorrillo Formation were mentioned by Feruglio (1945), who named this unit as “Dinosaur-bearing strata” because of the abundance of large bones of reptiles within these beds. Lately, an unnamed titanosaur was mentioned and illustrated in a popular book (Bonaparte, 1996). This specimen was commented in more detail by Bonaparte et al. (2002) who considered that because of its gracile proportions, it should be related to the genus *Aeolosaurus* (Powell, 2003). More recently Novas et al. (2019) described and analyzed

the fossiliferous content of Chorrillo Formation describing freshwater and terrestrial snails, silicified woods, palynomorphs, and a diverse vertebrate assemblage composed by fishes, anurans, snakes, turtles, indeterminate mammals, megaraptoran and unenlagiid theropod dinosaurs, the new sauropod *Nullotitan glaciaris*, the new ornithopod *Isasicursor santacrucensis*, and the ornithurine bird *Kookne yeutensis*. Afterwards, Chimento et al. (2020, 2021) reported the presence of the gondwanatherian mammal *Magallanodon baikashkenke* found in roughly coeval beds from Chile (Goin et al., 2020). More recently, Rozadilla et al. (2021) added the occurrence of ankylosaur and hadrosaurid remains from the Chorrillo Formation. In sum, the vertebrate record of the Chorrillo Formation includes indeterminate teleosts, calyptocephalellid frogs, indeterminate and madtsoiid snakes, chelid turtles, theropod and sauropod eggshells, the titanosaur sauropod *Nullotitan glaciaris*, and ornithischians including indeterminate ankylosaurs, the elasmarian ornithopod *Isasicursor santacrucensis* and hadrosaurs. There were also found megaraptorid and unenlagiid theropods, the ornithurine bird *Kookne yeutensis*, indeterminate mammals and the gondwanatherid *Magallanodon baikashkenke*.

These contributions indicate that the Chorrillo Formation exhibits early Maastrichtian vertebrate faunas associated with terrestrial environments that are similar to those extensively documented in northern and central Patagonia (e.g., Casamiquela, 1978; Leanza et al., 2004; Gasparini et al., 2015).

The goals of the present contribution are to define the paleoenvironmental conditions where the sediments of the Chorrillo Formation accumulated, to describe new vertebrate and plant remains and to include these, and previous findings within a stratigraphical frame, in order to give an integrated perspective of the sedimentology and paleontology of the lower Maastrichtian continental deposits of the Austral-Magallanes Basin at the Lago Argentino region. Furthermore, a detailed characterization of the sedimentology and paleontology of the Chorrillo Formation allow us to identify some regional stratigraphic correlations and make comparisons with other stratigraphic units of the basin.

2. GEOLOGICAL SETTING

The Austral-Magallanes Basin (AMB) is located on the southern part of Patagonia, including the most austral extension of both Argentina and Chile (Fig. 1). The tectonic history of the basin is divided into three main stages (Biddle et al., 1986; Arbe, 1989; Pankhurst et al., 2000; Fildani et al., 2003; Fosdick et al., 2011; Varela et al., 2012, 2019; Ghiglione et al., 2014; Malkowski et al., 2015; Calderón et al., 2016; Sickmann et al., 2018, 2019): i) An initial rifting stage, related with the onset of the Gondwana break-up, which took place from middle through Late Jurassic, resulting in the development of isolated grabens and half-grabens filled with volcaniclastic, volcanic and siliciclastic deposits of the El Quemado Complex (known as Serie Tobífera in Chile; Biddle et al., 1986); ii) a postrift, thermal subsidence stage that took place during the Tithonian-Albian, characterized by the transgressive and then regressive deposition of the Springhill and Río Mayer formations, (Biddle et al., 1986; Arbe, 1989; Rodriguez and Miller, 2005; Richiano *et al*., 2012, 2013, 2015, Poiré et al., 2017; Cuitiño et al., 2019); and finally iii) a compressional phase that took place during the Albian-Cenomanian times (~100 Ma) resulting in the development of a retroarc foreland system (Wilson, 1991; Fildani et al., 2003; Fosdick et al., 2011; Varela et al., 2012, 2019; Ghighlione et al., 2015; Malkowski et al., 2015, 2016, 2017; Sickmann et al., 2018).

During the beginning of the foreland stage the northern part of the AMB was divided into two main depocenters separated by the Piedra Clavada High (*sensu* Varela et al., 2019; Cuitiño et al., 2019): i) the main foredeep depocenter with a central axis orientated north-south from El Chaltén (Argentina) to Última Esperanza Region (Chile); and ii) the northeast-southwest oriented Cardiel-Tres Lagos depocenter (Varela et al., 2019).

The main foredeep depocenter is characterized by a clear overall regressive pattern. The onset of the foreland phase in the foredeep is marked by the deep-marine coarse-grained clastic turbiditic deposits of the Cerro Toro Formation (Kraemer and Riccardi, 1997; Cuitiño et al., 2019), which are overlain by the fine-grained slope system deposits of the Alta Vista Formation (also known as the Tres Pasos Formation in Chile; Romans et al., 2009; Hubbard et al., 2010;

Daniels et al., 2018; Auchter et al., 2020). Slope system deposits are overlain by the Campanian to Maastrichtian deltaic deposits of the La Anita Formation (equivalent to the lowermost interval of the Dorotea Formation in Chile; Macellari et al., 1989; Schwartz and Graham, 2015; Sickmann et al., 2018, 2019; Mánriquez et al., 2019; Moyano-Paz et al., 2018, 2020; Santamarina et al., 2020; Ghiglione et al. in press). During the late Campanian to Maastrichtian, the foredeep depocenter suffered a complete continentalization of the basin at the Lago Argentino region (Fig. 1) characterized by fluvial deposits grouped as the Upper Cretaceous Continental Deposits (UCCD *sensu* Tettamanti et al., 2018) which includes the Cerro Fortaleza, La Irene and Chorrillo formations (Moyano-Paz et al., 2018; Tettamanti et al., 2018; Sickmann et al., 2018, 2019; Ghiglione et al., in press). These fluvial deposits are overlain by the upper Maastrichtian deposits of the Calafate Formation across an erosive marine transgression surface (Macellari et al., 1989; Tettamanti et al., 2018; Odino-Barreto et al., 2018; Cuitiño et al., 2019; Rivera et al., 2020).

The Chorrillo Formation (Fossa Mancini et al., 1938; Feruglio, 1945), constituting the case study of this paper, crops out in the southern margin of the Lago Argentino. It overlies the braided fluvial deposits of the La Irene Formation and it is overlain by the marine transgressive deposits of the Calafate Formation (Fig. 1b; Macellari et al., 1989; Tettamanti et al., 2018; Odino-Barreto et al., 2018). The Chorrillo Formation consists mainly of reddish, greenish and grayish siliciclastic fine-grained sediments which alternate with greenish and yellowish conglomerate, pebbly-sandstone and sandstone bodies, and subordinate heterolithic deposits.

3. STUDY AREA AND METHODS

The study area is located southwest of the Santa Cruz province, southern Patagonia, Argentina, and it is known as the Lago Argentino region of the Austral-Magallanes Basin. The exposures of the Chorrillo Formation are restricted to the southern margin of the Lago Argentino and they constitute continuous outcrops for almost 30 km with a SW-NE orientation, from the gullies located at the south of the Alta Vista and Anita farms, until continuing its extension in

subsurface near the Calafate hill (Fig. 2). Toward the SW, the continuation of these deposits in Chile are known as part of the Dorotea Formation (Schwartz and Graham, 2015; Schwartz et al., 2017)

In order to carry out a general characterization and interpretation of the paleoenvironment involved in the deposition of the Chorrillo Formation, and to stratigraphically locate the recently discovered fossil content, this research included the measurement and description of a high-resolution stratigraphic section of ~500 m of the sediments that constitute the Chorrillo Formation, in the gullies of the Anita farm (Fig. 3). This methodology included the bed-by-bed description of thicknesses, mean grain size, sorting, and sedimentary structures present in the succession, as well as the survey of the position of paleontological findings. Then, a detailed analysis of sedimentary facies was carried out, allowing the interpretation of depositional processes (Table 1).

A detailed architectural analysis was performed, including the recognition and description of recurring appearance of facies groups, with characteristic vertical and lateral variations, contained within depositional bodies; as well as the detailed characterization of lithosomes geometries and dimensions, and their bounding surfaces. This allowed the definition of five architectural elements (e.g., Friend et al., 1979; Bridge, 1993; Gibling, 2006) interpreted as different sub-environments of the depositional paleoenvironment. The architecture of the studied deposits was determined by direct measurement, and by tracing of key stratal surfaces on scaled photopanels, and some parameters such as the width (W) / thickness (T) ratio were corrected for the obliquity of paleocurrents respect to the orientation of the outcrop belt. The external geometries of the channelized elements were described following the W/T criteria proposed by Gibling (2006). Finally, the fossil remains that were found within these deposits were stratigraphically located in the measured section.

The detailed description and interpretation of the different architectural elements and their spatial arrangement, together with the paleontological material provided valuable information about the sedimentary environment where these deposits accumulated.

Megafloristic remains were studied using a Nikon SMZ800 binocular microscope, photographed using a Canon Powershot SX540 HS digital camera, and assigned to different morphotypes. Terminology used for describing features of the leaves follows Ellis et al. (2009).

Institutional abbreviations. MPM-MIC, Colección Microfósiles, Museo Padre Molina, Río Gallegos, Santa Cruz province, Argentina; MPM-PB, Colección Paleobotánica, Museo Padre Molina, Río Gallegos, Santa Cruz province, Argentina; MPM-PV, Colección Paleontología de Vertebrados, Museo Padre Molina, Río Gallegos, Santa Cruz province, Argentina.

4. ARCHITECTURAL ELEMENTS

The Chorrillo Formation shows a maximum thickness of ~500 m in the study area (Fig. 3). Ten different lithofacies types were recognized in the Chorrillo Formation and are interpreted as having arisen via subaqueous unidirectional processes (confined and unconfined) or by pedogenic processes (Table 1). Sedimentary facies have been grouped into five facies associations representative of channelized and unchannelized fluvial deposition. Within these five facies associations, five architectural elements were recognized, each consisting of facies that occur in predictable vertical successions and geometric arrangements.

4.1 Complex sandy narrow sheets channels (SS)

Description: Architectural element SS displays forming lenticular sandstone bodies with conspicuous irregular concave-up lower boundaries and flat tops, and are up to 6 m thick and hundreds of meters of lateral continuity (Fig. 4A and B). The W/T ratios of SS elements range between 15 and 100 (narrow sheets channels *sensu* Gibling, 2006). Internally, it shows a complex organization defined by the vertical and lateral amalgamation of individual lenticular units, or storeys, up to 2 m thick and up to 30 meters wide (Fig. 4C). These storeys are

211 composed of medium- to coarse-grained sandstones with trough cross-bedding sets (St facies;
212 Fig. 4.d). Storeys may show mudstone rip-up clasts and wood fragments mantling the scouring
213 surface, conforming basal lags (Fig. 4D). Eventually, they may show fining-upward trends with
214 cross-bedded conglomerate facies (Gt) in the lower intervals of each storey.

215 *Interpretation:* This architectural element is interpreted as multistory fluvial channel deposits
216 where bedload was primarily transported as three-dimensional dunes at the bottom of the
217 channels and without the development of major cross-channel or marginal bars (Gibling, 2006;
218 Miall, 2006). The amount of amalgamated storeys inside these units suggests the development
219 of non-fixed channels that wandered across an alluvial plain, probably with a pattern of multiple
220 shallow channels and without the preservation of fine-grained floodplain facies due to
221 continuous lateral reworking (Veiga et al., 2007; Varela, 2015).

222 **4.2 Complex gravelly narrow sheets channels (GS)**

223 *Description:* Architectural element GS is characterized by external lenticular geometry with
224 erosional concave-up lower boundaries and flat tops. GS bodies are up to 6 m thick and
225 hundreds of meters of lateral continuity. The W/T ratios of the bodies of this architectural
226 element ranges between 15 and 100 (narrow sheets channels *sensu* Gibling, 2000). GS is
227 characterized by a complex internal organization defined by the cyclic alternation between thin
228 sandy up to 0.2 m thick and gravelly beds which are up to 1.5 m thick, limited to each other by
229 net boundaries (Fig. 5). Sandy beds may show trough cross-bedding (St) or ripple lamination
230 (Sr) structures, while masive to trough cross-bedding gravelly layers consist of Gm or Gt facies
231 (Fig. 5).

232 *Interpretation:* This architectural element (GS) is interpreted as sandy-gravel bed-load
233 multistory fluvial channels, infilled by migration and downstream accretion of three-
234 dimensional dunes and bars. Bars can be simple (formed by sets) or compound (formed by
235 cosets) and both suggest downstream direction of accretion (Bridge, 2003; DA downstream
236 accretion bars *sensu* Miall, 1996, 2006). It ss interpreted that these bars were not attached to a

channel margin, because no lateral accretion component was recognized. GS architectural element reflects deposition of gravel and sand in diluted conditions from multiple channels within a main channel belt (Bridge et al., 2000; Tettamanti et al., 2018).

4.3 Sandstone lobes (SL)

Description: The deposits that constitute this architectural element are characterized by an external lenticular geometry with a faint basal surface, given by the gradual increase in grain size from the fine-grained deposits of FG element (Fig. 6A), and a convex-up top (Fig. 6B). The thickness of these lens-shaped units ranges between 2 and 4 m and their lateral extent is in the order of tens to few hundred meters. These bodies usually define coarsening and thickening upward trends composed of fine- to very coarse-grained sandstones. Each sandstone layer can reach up to 1 m thick, and internally shows horizontal lamination which grades upward into trough cross-bedding or ripple lamination structures (Sh, St and Sr facies, respectively). Convolute laminated sandstones and massive sandstone beds were also recorded within these bodies. Within the architectural element SL, crocodile and Megaraptoridae fossil remains were found (Fig. 3).

Interpretation: These lobate bodies with coarsening and thickening upward trends, closely related to floodplain deposits (FG architectural element) can be interpreted as the result of the progradation of crevasse splays, related to overbank flows close to main fluvial channel margins (Smith et al., 1989; Clemente and Pérez-Arlucea, 1993; Veiga et al., 2007); while the horizontal laminated sandstones (Sh) indicate upper flow regime conditions during splay flood events. The overlying lithofacies St and/or Sr suggest a subsequent reduction in flow energy (Bristow et al., 1999; Yeste et al., 2020). The occurrence of syn-sedimentary deformation and massive beds reflect rapid sediment accumulation onto a water-saturated substrate (Rossetti and Santos, 2003; Owen and Santos, 2014; Burns et al., 2017; Yeste et al., 2020).

4.4 Thick reddish fine-grained deposits (FG)

Description: This architectural element is composed of reddish and greenish massive mudstones that occasionally intercalate with sandstone beds (Fig. 7A). The geometry of these deposits is tabular, with horizontal and sharp bounding surfaces. Facies packages range in thickness from a few centimeters up to 30 m and may be up to 1000 m in lateral extent. Mudstone deposits (Fm facies) are characterized by abundant pedofeatures such as rhizoliths (Fig. 7B), mottles, cutans, and slickensides (Fig. 7C); and by granular and subangular to angular blocky peds as the main pedogenic structures (Fig. 7D). Sandstone deposits form tabular or lenticular thin beds up to 0,5 m thick and tens of meters of lateral extent which are eventually intercalated. Tabular sandstone beds consist of Sh facies; while lenticular beds may show Sh, St, and Sr facies. Within the architectural element FG, abundant plant debris, chondrichthyan, Hydromedusinae, Meiolaniformes, *Isasicursor santacrusensis*, hadrosaur, ankylosaur, titanosaur, Megaraptoridae, Enantiornithine, *Kookne yeutensis* and Gondwanatheria fossil remains were found (Fig. 3).

Interpretation: These deposits are interpreted to record sedimentation of mud by suspension fallout, and via deposition of mud traction load sand-grade and silt-grade aggregates of mud-sized particles that, through later compaction, were restructured into a mudstone texture (Wright and Marriot, 2007; Wakelin-King and Webb, 2007; Dasgupta et al., 2017; Coronel et al., 2020). Therefore, this architectural element is interpreted as a deposition in a floodplain sub-environment characterized by widespread paleosol development; where the greenish colored deposits with hydromorphic pedofeatures (gley mottles and rhizoliths) indicates seasonal poor drainage conditions (Retallack, 2001; Varela et al., 2012b). While the reddish ones suggest good drainage conditions (Varela et al., 2012, 2019). Episodic unidirectional tractive flows with variable degree of channeling are interpreted to be responsible for deposition of sandstone beds, and could be related to the distal expression of crevasse-splays deposits and small scale floodplain channel deposits (Yeste et al., 2020).

4.5 Thin dark fine-grained deposits (DF)

Description: The deposits that constitute this architectural element form tabular geometries with horizontal and sharp bounding surfaces. These deposits thicknesses may range from several centimeters up to 10 m and may reach up to 100 m of lateral extension. Internally, these elements are composed of organic-rich grey, dark grey to dark purple thin-laminated mudstones (Fl; Fig. 7E) with abundant well preserved plant remains (Fig. 7F and G). Sporadic, thin, massive limestones and massive mudstone lamina also occur without pedofeatures. Within the architectural element DF, Pipoidea, *Calyptocephalella* sp, Anilioidea, *Rionegrophis* sp., Hydromedusinae, Enantiornithine, Gondwanatheria and titanosaur fossil remains were found (Fig. 3).

Interpretation: Deposits of this architectural element reflect deposition by settling from suspended load in a low-energy environment. The grey, dark grey and dark purple colors, as well as the abundant poorly decomposed organic matter and the absence of biogenic structures, suggest reducing and anoxic conditions (Everett, 1983; Yeste et al., 2020; Varela et al., 2021). This architectural element is interpreted as accumulated in a water-logged, swamp-like environment (Yeste et al., 2020; Varela et al., 2021).

5. PALEONTOLOGICAL CONTENT

The Chorrillo Formation deposits carry several beds with abundant fossil content including megafloristic remains, palynomorphs, vertebrate and invertebrate remains. Novas et al. (2019) presented the first descriptions of these materials. In this work, we locate stratigraphically the described fossils by Novas et al. (2019) and incorporate descriptions of newly collected materials (Fig. 3).

5.1 Paleobotany

Continental plant remains have been recovered from Chorrillo Formation beds. The first report came from the lowermost interval of the unit, near the stratigraphic contact with the La Irene Formation (Novas et al., 2019). Reports include conifer fossil woods (*Podocarpoxylon dusenii* Krausel 1924) and palynological assemblages showing moderate specific diversity, represented

313 by lycopods, different fern families (e.g., Dicksoniaceae, Osmundaceae, Gleicheniaceae),
314 Podocarpaceae, and some angiosperm taxa (e.g., *Peninsulapollis gilli* (Cookson) Dettmann et
315 Jarzen 1988, *Clavatipollenites* sp., *Tricolpites reticulatus* Cookson 1947 ex Couper 1953;
316 Novas et al., 2019). Here we present descriptions of two new beds with plant remains in order to
317 improve the knowledge of the Late Cretaceous vegetation of the basin.

318 Within the architectural element FG deposits at 215 m in the stratigraphic column (Fig. 3)
319 abundant plant debris preserved as impressions/compressions was found. The most conspicuous
320 element are fragments of leaves with parallel veins showing two ranked (major and minor) veins
321 (Morphotype 6; Fig. 8A), which are probably related to monocots. Small fragments of
322 dicotyledonous leaves (~5 mm) were also recognized. A single specimen shows a stout midvein
323 with lateral veins diverging that produce several dichotomies at the same level (Fig. 8B) before
324 reaching the margin. Several specimens lack a midvein, presenting radiating veins that
325 dichotomize 3-4 times at comparable levels, being the last dichotomies located near the margin
326 and ending in a loop (Fig. 8C and D). Both types of elements, with and without midveins, show
327 a regular reticulum of low rank veins present between principal veins.

328 The similar patterns of dichotomies in the lateral/major veins, and the irregular reticulum
329 suggest that they may be part of the same type of leaf. Venation patterns are closely comparable
330 with the ones observed in Nymphaeales (Taylor and Gee, 2014; Gee and Taylor, 2019), a clade
331 of aquatic plants present in the fossil record since the Early Cretaceous (Taylor and Gee, 2014;
332 Gee and Taylor, 2019). The interpretation of seasonally waterlogged, temporary swamp-like,
333 environment of the architectural element FG is consistent with the aquatic nature of these plants.

334 Additional plant impressions were collected from the architectural element FG at 295 m in the
335 stratigraphic column (Fig. 3). Within these deposits five different morphotypes were
336 recognized, including dicots (Morphotypes 1, 2, 3 and 4; Fig. 8E-J) and monocots (Morphotype
337 5; Fig. 8K), along with root remains (Fig. 8L). The most abundant element is defined here as
338 Morphotype 1 (Fig. 8E-G), and comprises elliptic asymmetric leaves with pinnate primary
339 venation and brochidodromous secondary venation and looped exterior tertiaries.

A leaf similar to Morphotype 1 was illustrated by Ortuya et al. (2016), who found it at the base of the coeval Dorotea Formation (Chile), and that was referred as *Coccoloba?* sp. However, this specimen has not been described yet, and detailed comparisons are still needed. Moreover, similar leaves were reported by Berry (1938) for the Eocene Pichileufu assemblage of the Huitrera Formation, and were referred to *Coccoloba ruizianiformis*, in reference to the similarities with the extant species *Coccoloba ruiziana* of the Polygonaceae. However, beyond the gross similarities in external morphology, it is important to note that in absence of more informative remains (e.g., flowers, fruits), a conclusive referral to the modern genus is not certain. Additionally, age estimates for the divergence of the Coccolobeae clade place its origin during the latest Paleocene-earliest Eocene (Schuster et al., 2013).

The remaining leaf morphotypes are very fragmented. Morphotype 2 is the only recognized morphotype having palmate primary venation, but given its fragmentary nature, few anatomical traits can be recognized (Fig. 8H). Leaves with palmate venation have been reported from the Dorotea and Tres Pasos Formations at Chile, and were referred to the genus *Brachychiton*, and to "*Sterculia" sehuensis* Berry (Ortuya et al., 2016; Yabe et al, 2006; Lobos et al., 2018; Manríquez et al., 2019), and some fragmentary remains (Kurtz, 1899; Hunicken, 1971). Morphotype 3 consists of a partial leaf which preserves its acute apex and primary vein with decurrent secondaries (Fig. 8I). Morphotype 4 shows a straight midvein with a pinnate pattern, with non-decurrent secondaries arising in acute angles (Fig. 8J). Finally, Morphotype 5 includes fragments of leaves with one-ranked parallel veins (Fig. 8K), that may fall within the broad fossil genera *Eolirion* Schenk 1869 or *Palmophyllum* Conwentz 1886, both of unclear taxonomic affinities.

5.2 *Vertebrate fossils*

364 The preliminary vertebrate faunal list offered in previous papers (Novas et al., 2019; Chimento
365 et al., 2020, 2021; Rozadilla et al., 2021) is here expanded with the addition of new fossil
366 remains of already reported taxa as well as the first record for some clades.

367

368 **6. SYSTEMATIC PALEONTOLOGY**

369 Chondrichthyes Huxley 1880

370 Lamniformes Berg 1958

371 Genus and species indeterminate

372 **Referred material**. MPM-PV-22839, isolated upper lateral tooth lacking the roots (Fig 9A).

373 *Provenance*: MPM-PV-22839 was found at the *Isasicursor* II Site related with the architectural
374 element FG deposits (Fig. 3).

375 *Description*: MPM-PV-22839 is represented by a subtriangular crown, devoid of serrations and
376 lacking additional cusplets. The crown is slightly mesially oriented and lacks striations. The
377 labial face is slightly convex transversely. The cutting edges extend along the mesial and distal
378 margins of the crown. In labial view, there exists a poorly defined concavity separating the
379 crown from the root. In mesial and distal views, the crown shows a poorly defined sigmoid
380 curvature (Fig. 9A).

381 *Comments*: MPM-PV-22839 shows a simple crown with a large subtriangular cusp, with
382 extended mesial and distal cutting edges and a sigmoidal survature when viewed from the sides,
383 a combination of characters typical of lamniform sharks (Cappetta, 2012). The specimen here
384 described is too incompletely preserved and precludes a referral to generic level. The shape of
385 the crown is reminiscent to the genera *Carcharias* and *Cretalamna*, the latter reported from the
386 Latest Cretaceous Calafate and Cerro Fortaleza Formations at Santa Cruz province (Schroeter et
387 al., 2014; Bogan et al., 2017).

This constitutes the first finding of a chondrichthyan from the Chorrillo Formation. The incomplete and eroded nature of this specimen may indicate that it belongs to beds of the overlying Calafate Formation that previously yielded several shark teeth (Bogan et al., 2016, 2017). Previous reports of fishes from Chorrillo Formation include crushing teeth of indeterminate teleosts (Novas et al., 2019). This tooth is lanceolate in shape, with a translucent cap having acute mesial and distal carinae. However, this combination of characters is also present in other fish clades (e.g., lepisosteiforms), and thus, the specimen should be regarded as an indeterminate actinopterygian.

Anura Fischer von Waldheim, 1813

Pipoidea Gray, 1825

Genus and species indeterminate

Referred material. MPM-PV-22840, distal end of right humerus (Fig. 10A-C).

Provenance: the specimen was found at *Magallanodon* Site, from deposits of the architectural element DF (Fig. 3).

Description: MPM-PV-22840 has a prominent humeral ball, which is subspherical in shape and is relatively small, with a transverse diameter that is a little more than half of the maximum width (0.52 mm) of the distal end of the humerus (Fig. 10C). The proximodistal axis of the articular ball coincides with the proximodistal extent of the humeral shaft. The ventral cubital fossa is poorly defined and is centrally located (Fig. 10A). The olecranon fossa is crescent-shaped, transversely wider than proximodistally long, and with well-defined margins. It is centrally located with respect to the main transverse axis of the distal end of humerus. Epicondyles are subtriangular in shape and extend distally, resulting in a roughly symmetrical distal end of the bone (Fig. 10B). The medial epicondyle is slightly longer than the lateral one, and both reach the level of the distal margin of the humeral ball. The medial epicondyle is

separated from the humeral ball by a notch and in posterior view shows a proximal ridge that reaches the olecranon fossa. The shaft walls are thick and the medullary cavity is very small.

Comments: MPM-PV-22840 may be referred to Pipoidea on the basis of relatively thick humeral walls, a roughly symmetrical distal end with distally extended epicondyles, a crescent-shaped, proximodistally short and centrally located olecranon fossa, a prominent, relatively small and subspherical humeral ball, and a prominent lateral epicondyle (Estes and Reig, 1973; Baez, 1987; Gao and Wang 2001; Worthy et al., 2013; Gómez, 2016). The well-defined ventral fossa and roughly symmetrical distal end distinguishes this specimen from species of the extant pipoid genus *Xenopus* (Baez, 1987). However, the incomplete nature of MPM-PV-22840 forbids detailed comparisons with other extinct or extant pipoids.

Neobatrachia Reig 1958

Calyptocephalellidae Reig 1960

Calyptocephalella Duméril and Bibron 1841

Calyptocephalella sp.

Referred material. MPM-PV-22841, incomplete left maxilla (Fig. 10D-E); MPM-PV-22842, incomplete right maxilla (Fig. 10F-G); MPM-PV-22843, incomplete right ilium (Fig. 10J-K); MPM-PV-22844, proximal right radioulna (Fig. 10H-I); MPM-PV-22845, left proximal end of tibiofibula (Fig. 10L-M); MPM-PV-22846, proximal half of urostyle (Fig. 10).

Provenance: the specimens were found at *Magallanodon* Site, from deposits of the architectural element DF (Fig. 3).

Description: MPM-PV-22841 and MPM-PV-22842 are poorly preserved maxillae and show incomplete anterior and posterior ends (Fig. 10D-E). Most of the external surface of the bones is

ornamented by deep subcircular pits separated by bony ridges, with the exception of MPM-PV-22842 in which the alveolar margin is smooth.

The lateral surface of the bone is strongly convex. In the case of MPM-PV-22842 (Fig. 10F-G) this surface is separated from the alveolar margin by a longitudinal ridge. The smooth alveolar margin is anteriorly tall and becomes lower towards the posterior end of the bone. In medial view the palatine shelf is step-like, robust and prominent, well separated from the maxillary body.

The *pars dentalis* is dorsoventrally deep and shows the preserved base of the teeth that are subvertically oriented and are subparallel to each other. The bases indicate that each tooth root was ankylosed to the maxilla, conforming typically pedicellate dentition, as is diagnostic for Neobatrachia (Reig 1958).

MPM-PV-22843 is an incomplete right ilium (Fig. 10J-K) belonging to a very small individual. In medial view it shows a very deep and well defined oblique groove and crista (*sensu* Rocek. 2013). The contact for the opposite ilium is relatively wide, subcircular in contour and notably concave. In spite of deficient preservation the supracetabular and subacetabular expansions were well-developed. The dorsal tubercle is represented by an elongate protuberance forming an anteriorly extended dorsal crest. This crest barely reaches the level of the anterior margin of the acetabulum and is laterally concave. The acetabulum is prominent with a well-defined and acute delimiting edge. The iliac shaft-subacetabular extension forms an angle greater than 90º.

MPM-PV-22844, is an incomplete proximal end of a right radioulna (Fig. 10H-I). The bone is stout, with a transversely compressed shaft. The preserved portion indicates that it was a short and robust element with expanded distal end (as shown by the distally divergent anterior and posterior margins). The bone shows a tall, and thick olecranon process. In lateral view there is a conspicuous nutritive foramen close to the proximal articular surface.

460 The proximal end of tibiofibula (MPM-PV-22845) is relatively robust (Fig. 10L-M). The anterior and
461 posterior grooves are poorly defined and relatively narrow. The proximal end of tibia is convex and
462 prominent, and is separated from the lateral fibular process by a concave surface. The fibular process
463 is relatively narrow and proximodistally extensive.

464 The preserved portion of urostyle (MPM-PV-22846) indicates a robust element that was relatively
465 short, judging by the degree of convergence of the margins of the bone. As in other neobatrachians
466 the urostyle lacks transverse processes and exhibits a bicondylar proximal articulation (Gómez et al.
467 2011). The proximal articular surfaces are dorsoventrally tall and suboval in contour. The dorsal
468 longitudinal crest of the urostyle is represented by a transversely thickened base. Ventrally, the
469 urostyle shows a poorly defined longitudinal crest.

470 *Comments*: The maxillae MPM-PV-22841 and MPM-PV-22842 are referred to Calyptocephalellidae
471 by having an external ornamentation composed by pits and ridges, dorsoventrally tall *pars dentalis*,
472 well-developed and laminar pterygoid process, alveolar margin and step-like palatine shelf, and
473 ascending process subvertically oriented and laminar in cross-section (Casamiquela 1958; Báez and
474 Gasparini 1977; Gómez et al. 2011; Agnolín 2012). Because of the incomplete nature of the
475 specimens, we refer to the material as *Calyptocephalella* sp. (Fig. 10D-G).

476 The ilium MPM-PV-22843 (Fig. 10J-K) shows a combination of characters present in
477 *Calyptocephalella*, including dorsal prominence that extends anteriorly as a dorsal crest, the later one
478 rising from the shaft and showing a longitudinal concavity in lateral view, the angle between the
479 subacetabular process and the iliac shaft is wider than 90º, and presence of prominent oblique groove
480 and crest in medial view (Báez, 1987). Consequently, the specimen is here referred to the genus
481 *Calyptocephalella*.

482 The available postcranial bones are notably robust and stout, as also occurs in Calyptocephalellidae
483 (Reig, 1960). All are congruent in morphology with extant *Calyptocephalella gayi*. The robustness
484 and the anteroposterior shortening of the urostyle (MPM-PV-22846) are features typical of
485 Calyptocephalellidae (Reig 1960; Agnolín 2012). The specimen differs from *Gigantobatrachus* by

being much smaller, and by having roughly symmetrical proximal articular surfaces (Casamiquela 1963).

Available calyptocephalellid material indicates the coexistence of two different-sized taxa, based on morphological differences noted in the maxillae. as well as body size (a species very small in size and another form close in size to extant species *Calyptocephalella gayi)*. Because of the incomplete and isolated nature of the material, it is uncertain if they belong to different taxa or to different ontogenetic stages. However, the differences noted between the available maxillae indicate that they may pertain to specifically different taxa.

Squamata Oppel, 1811

Serpentes Linnaeus, 1758

Anilioidea Fitzinger, 1826

Genus and species indeterminate

Referred material. MPM-PV-22847, possible mid-precloacal vertebra (Fig. 11A-D).

Provenance: the specimen was found at *Magallanodon* Site, from deposits of the architectural element DF (Fig. 3).

Description: The specimen is poorly preserved and shows incomplete anterior surface and neural arch. However, the preserved portion of the neural arch indicates that it was notably depressed and exhibited a transversely wide neural canal (Fig. 11C). The postzygapophyseal process is short and transversely narrow.

In ventral view the centrum is subtriangular in contour, with a well-defined haemal keel separated by deep and wide subcentral depressions (Fig. 12A). A pair of subcentral foramina is present. The subcentral depressions are delimited by well-developed and straight subcentral ridges.

509 *Remarks*: This vertebra may be referred to Anilloidea on the basis of the following combination of
510 characters: depressed vertebrae with low neural arch, vertebral centra subtriangular in contour when
511 viewed ventrally, being notably broader anteriorly than posteriorly (Rage, 1998; Gómez et al., 2008).
512 Poor preservation of the vertebra precludes a taxonomic assignment beyond Anilioidea. In any case,
513 the element differs from the Maastrichtian anilioid *Australophis* from Rìo Negro province in having
514 vertebral centrum that is notably broader anteriorly (Gómez et al., 2008).

515 Anilioidea have been traditionally considered a distinct lineage to comprise the most basal forms
516 among living snakes (Rieppel, 1988). The extant South American *Anilius* Oken, 1816 and Asian
517 *Anomochilus* Berg, 1901, *Cylindrophis* Wagler, 1828 and the uropeltids, as well as several extinct
518 taxa, have been referred to this lineage (Rage, 1984). However, in recent morphology-based
519 phylogenetic analyses of snakes (e.g., Rieppel, 1988; Kluge, 1993; Cundall et al., 1993; Tchernov et
520 al., 2000; Lee and Scanlon, 2002; Vidal and Hedges, 2002, 2004; Wilcox et al., 2002; Gower et al.,
521 2005), the taxa traditionally recognized as anilioids are interpreted as basal to all other
522 alethinophidians, and not always recovered as a monophyletic.

523 To date four extinct genera based on isolated vertebrae, have been ascribed to Anilioidea in South
524 America: *Coniophis* and *Hoffstetterella* from the Palaeocene of northern South America,
525 *Colombophis* from the middle Miocene of Colombia (Hoffstetter and Rage, 1977; Rage, 1998), and
526 *Australophis* from the Maastrichtian of northern Patagonia (Gómez et al. 2008). Present discovery
527 constitutes the southernmost for the entire group and also the first Anilioidea for the Austral-
528 Magallanes basin.

529

530 "Madtsoiidae" Hoffstetter, 1961

531 cf. *Rionegrophis* sp.

532 **Referred material**. MPM-PV-22848, incomplete centrum of trunk vertebra (Fig. 11E-F).

Provenance: the specimen was found at *Magallanodon* Site, from deposits of the architectural element DF (Fig. 3).

Description: MPM-PV-22848 consists of a fragmentary vertebral centrum including most of the posterior articular ball. It corresponds entirely in size and shape to an incomplete vertebra previously described by Novas et al. (2019). The articular ball is prominent, sub-circular shaped in posterior view, and slightly dorsally pointed. The ventral surface of the centrum exhibits a haemal keel on its posteriormost region, being flanked by two small concavities representing the posterior end of the subcentral depressions. Subcentral ridges are present.

Remarks: The specimen is very similar in size and shape to with that reported from the Chorrillo beds cf. *Rionegrophis madtsoioides* by Novas et al. (2019). Due to the fragmentary nature of MPM-PV-22848, comparisons are limited. However, its relatively large size and robust proportions resemble *Rionegrophis*. It shares with *Rionegrophis madtsoioides*, the type species of the genus coming from Maastrichtian beds at northern Patagonia (Albino,1987, 1995), a well-developed and narrow haemal keel, well-defined subcentral ridges and a roughly subtriangular-shaped centrum when viewed dorsally or ventrally (Novas et al., 2019). However, the fragmentary nature of specimens coming from Chorrillo Formation makes a generic referral tentative. In this way we regard all specimens from this unit as cf. *Rionegrophis*.

Testudines Linnaeus 1758

Pleurodira Cope 1865

Chelidae Gray 1825

Hydromedusinae Georges et al. 1998 sensu Joyce et al. 2021

Genus and species indeterminate

Referred specimens: MPM-PV-22849, left peripheral 3 or 4 (Fig. 12A–D); MPM-PV-22850, bridge peripheral (Fig. 12E, F); MPM-PV-22851, fragment indet. (Fig. 12G–I); MPM-PV-22852 bridge peripheral (Fig. 12J, L); MPM-PV-22853, right hypoplastron (Fig. 12M,N); MPM-PV-22854, buttress (Fig. 12O); MPM-PV-22856, plastral fragment (Fig. 12P–Q); MPM-PV-22855, ?plastral fragment (Fig. 12R).

Provenance: the specimens were found within the deposits of the architectural elements DF and GF, exposed at the*Magallanodon* Site, *Isasicursor* I Site, and *Isasicursor* II Site (Fig. 3).

Description: All the plates described herein show similar ornamentation patterns formed by irregular polygons of different sizes. This ornamentation pattern is known in the South American long-necked lineage Hydromedusinae formed by *Hydromedusa* spp.-*Yaminuechelys* spp. Usually, *Hydromedusa* spp. do not exceed the carapace size of 30–40 cm, while adult *Yaminuechelys* spp. are 40 cm to 80 cm long.

MPM-PV-22849 (Fig. 12A–D) is identified as a peripheral 3 or 4 because in the ventral surface the scar for the axillary buttress is preserved. In dorsal view, the sulcus delimiting consecutive marginal scutes and the sulcus between marginals and pleural scutes indicate that, at least anterior marginal scutes were restricted to peripheral bones. MPM-PV-22850 and MPM-PV-22851 (Fig. 12E,F, J-L) represent a bridge peripheral. Two sockets for the ribs (dorsal) and two or three sockets for the pegs of the hyo-hypoplastron are preserved in medial view in MPM-PV 22852, indicating that the connection between the carapace and plastron was through ligaments.

MPM-PV-22853 (Fig. 13M-N) preserves the base of the inguinal buttress and in ventral view, the abdomino-femoral sulcus is preserved.

Remarks: As indicated previously (Novas et al., 2019) most available turtle material from the Chorrillo Formation is congruent with the presence of a single chelid taxon along the stratigraphical column. The specimens here described may be identified as belonging to Chelidae by having the combined presence of pelvic scars in the carapace, free peripheral plates

581 which lack of firm contact with costal plates, and external surface decoration consisting of
582 dichotomizing sulci and polygones (Broin and de la Fuente, 2001; Lapparent de Broin, 2003).
583 The material is too incompletely preserved to allow a clear generic referral. The ornamentation
584 is very similar to that described for the Hydromedusinae, which includes the genera
585 *Yaminuechelys* and *Hydromedusa* (see Alarcón-Muñoz et al. 2020). Both genera share with the
586 specimens here described the ornamentation made up by polygons having three or more well-
587 defined sides and many of them are markedly elongated (see Alarcón-Muñoz et al. 2020). The
588 specimens here described are indistinguishable from those described from the coeval Dorotea
589 Formation as belonging to *Yaminuechelys* (Alarcón-Muñoz et al., 2020). However, a generic
590 referral is not clear, and the available material from the Chorrillo Formation represents a taxon
591 much smaller in carapace length than the known *Yaminuechelys* species, being similar in this
592 aspect to the genus *Hydromedusa*. Consequently, they are referred here as Hydromedusinae gen.
593 et sp. indet., until more material becomes available.

594

595 Meiolaniiformes Sterli and de la Fuente 2013

596 Genus and species indeterminate

597 **Referred specimens**: MPM-PV-22858, distal end of a left humerus (Fig. 13).

598 *Provenance*: the specimen was recovered from deposits with architectural element FG, exposed
599 in *Isasicursor* II Site (Fig. 3).

600 *Description*: The distal end of humerus is expanded, preserving both the ectepicondyle and
601 entepicondyle (Fig. 13A). The ectepicondyle bears an enclosed ectepicondylar foramen in
602 dorsal view. In ventral view, the condyles for the articulation with the radius (capitellum) and
603 with the ulna (trochlea) are well-defined (Fig. 13C). The trochlea is bigger than the capitellum
604 as occurs in *Peligrochelys* (Sterli and de la Fuente, 2019).

Remarks: The Cretaceous record of continental turtles in Southern South America is represented by the basal meiolaniforms and two main pleurodiran clades, the chelids and the pelomedusoids (Vlachos et al. 2018). Based on the fossil record and on the morphology observed in the humerus described herein (e.g., enclosed ectepicondylar foramen, well-developed condyles for radius and ulna), we assign it to the clade Meiolaniformes. The morphology of this humerus is reminiscent of unpublished humeri from La Colonia Formation of Chubut Province (JS pers. obs.). The meiolaniiform specimen described above currently represents the southernmost record for the clade in South America.

Sauropterygia Owen, 1860

Plesiosauria de Blainville, 1835

Elasmosauridae Cope, 1869

Genus and species indeterminate

Referred material: MPM-PV-22859 incomplete cervical centrum and the lateral half of a very fragmentary dorsal vertebra (Fig 11G-J).

Provenance: the isolated and heavily weathered centra were collected come from upper terms of Chorrillo Formation, but they almost probably fell from the underlying marine deposits of the Calafate Formation (Fig. 3).

Description: MPM-PV-22859 includes an incomplete centrum from the anterior region of the neck (Fig 11G-H) and a dorsal centrum (Fig 11I-J). The ventral surface of the cervical centrum shows paired subcentral foramina. These are subcircular in shape and approximately 5 mm long. There is a short longitudinal keel between the foramina. The cervical ribs are not fused to the centrum and the parapophyses are displaced towards the ventral region. The parapophysial articular face is bilobed and slightly concave.

629 The dorsal vertebra is represented only by an incomplete centrum. The neural arch was not
630 fused to the center. In the ventral surface, a small subcircular nutritive foramen is observed. The
631 centrum articular surfaces are nearly flat.

632 *Remarks*: The presence of a concavity at the ventral surface of the cervical centrum and a
633 ventral notch on the articular faces of the cervical vertebra, resulting in bilobed-contour is
634 diagnostic of the clade Euelasmosaurida (O'Gorman, 2020). The presence of a pair of nutritive
635 subcentral foramina is a character typical of plesiosaurs (Benson & Druckenmiller, 2014). The
636 fragmentary and isolated nature of the specimens precludes a taxonomic referral beyond the
637 family level. It is worth mentioning that the size of the cervical centrum indicates a plesiosaur of
638 relatively small size, similar to *Kawanectes* (O'Gorman, 2016).

639 The marine Calafate Formation, previously yielded plesiosaur specimens (Fig. 3; D´Angelo et
640 al., 2016). Furthermore, plesiosaur remains have been recovered from the upper layers of the
641 Chilean Dorotea Formation (Otero et al., 2015; Manríquez et al., 2019), which may be
642 correlated with the Calafate Formation.

643

644 Dinosauria Owen, 1842

645 Ornithischia Seeley, 1887

646 Ornithopoda Marsh, 1881

647 Elasmaria Calvo et al., 2007

648 *Isasicursor santacrucensis* Novas et al., 2019

649 **Referred materials:** MPM-PV-22860 a fragmentary right maxilla with a complete maxillary
650 teeth (Fig. 14A-B); MPM-PV-22861 the proximal end of a right ulna (Fig. 14C-G); MPM-PV-
651 22862 a left metatarsal III (Fig. 14H-L).

Provenance: The specimens were found within the deposits of the architectural element FG referred as *Isasicursor* Site II (Fig. 3).

Description: Many of the newly discovered materials overlap with those originally described by Novas et al. (2019), allowing us to determine the remains as belonging to *Isasicursor santacrucensis*. Therefore, we here describe some selected materials that shed new insights on the anatomy of this dinosaur.

MPM-PV-22860 consists of an incomplete right maxilla, preserving several maxillary teeth (Fig15A-B). The lateral surface of the maxilla is smooth, and shows part of an ovoidal antorbital fossa on its dorsal half. Ventral to the antorbital fossa, the maxilla is laterally convex. In ventral view the dental row is straight and inset medially. There are 7 teeth tooth positions, only one preserving its crown. The maxillary tooth root is ovoidal in cross-section. The maxillary teeth crown has a rhomboidal outline. In labial view, it shows a primary ridge separating the crown asymmetrically, with a wider posterior portion. The primary ridge defines the apex of the maxillary teeth. Several secondary ridges run apicobasally in the anterior and posterior halves of the lingual surface. There is a single ridge in the anterior half and 3-4 ridges in the posterior half of the crown. The lingual surface of the crown is concave and lacks ornamentation.

The proximal end of a right ulna (MPM-PV-22861) was recovered (Fig. 14C-G). In proximal view, the ulna is sub triangular in cross-section, with a convex lateral margin, and concave medial and anterior margins. The medial process is more developed than the lateral one. The medial process projects anteromedially; it is subrectangular in proximal view, and subtriangular in medial view. On the other hand, the lateral process is subtriangular in anterior proximal and lateral views. Between these processes there is a narrow depression for articulation with the radius. The posterior surface is posteriorly bowed and bears a thick ridge that ends proximally in the olecranon, which is subtriangular in cross-section. The lateral surface of the bone is flat, while the medial one is deeply concave.

A nearly complete left metatarsal III (MPM-PV-22862) is available (Fig. 15H-L). It lacks the proximal end and part of the shaft. The preserved proximal end is ornamented by longitudinal stripes. The bone shaft is subrectangular in cross section. Its anterior surface is concave, especially on its mid length. The anterior surface of the bone is delimited by sharp lateral and medial ridges that project anteriorly. In lateral view, the shaft tapers distally. The lateral surface bears an oblique ridge that runs anteroproximally to posterodistally. This oblique ridge divides the lateral surface in a proximal and concave half from a distal and convex half. The medial surface is flat and straight. The posterior surface is proximally distorted and shows a medial margin that is more posteriorly projected than the lateral one. Its distal end shows an asymmetrical distal trochlea. The articular surface is well defined by a sulcus. The distal condyles are separated by a well-developed intercondylar groove. In distal view, the condyles are asymmetrical, the medial one being larger than the lateral one. The lateral surface of the bone has a deep and sub-circular collateral pit, while the medial one is shallower.

Remarks: We here describe the first cranial remains of *Isasicursor santacrucensis.* As in other Gondwanan elasmarians, such as *Talenkauen, Anabisetia,* and *Gasparinisaura,* the maxillary teeth are asymmetrical and with a well-defined primary and secondary ridges (Coria and Salgado, 1996; Coria and Calvo, 2002; Novas et al., 2004; Rozadilla et al., 2019). The ulna of *Isasicursor* has a concave medial margin in proximal view, being different from the straight condition present in *Mahuidacursor* and *Anabisetia* (Coria and Calvo, 2002; Cruzado-Caballero et al., 2019), but similar to *Notohypsilophodon* (Martinez, 1998; Ibiricu et al., 2014). On *Isasicursor* the medial process of proximal ulna is medially projected while in *Mahuidacursor* it is more anteriorly extended. The metatarsal III of *Isasicursor* is a long but stout element, being proportionally transversely wider than in *Anabisetia* and *Morrosaurus* (Coria and Calvo, 2002; Rozadilla et al., 2016), resembling the condition described for *Talenkauen* (Rozadilla et al., 2019).

Remains discovered of *Isasicursor* from *Isasicursor* Site II (Fig. 14) consist of several individuals corresponding to different ontogenetic stages (Fig. 15). They are represented by

diverse juvenile and adult individuals, including a notoriously big specimen (Fig. 15A). The same occurs with previous findings of this species at *Isasicursor* Site I (Fig. 3), previously reported by Novas et al. (2019). It is worth mentioning that most *Isasicursor* remains recovered at the *Isasicursor* Site I and Site II roughly represent the same elements: long bones of the hindlimb and sacral and caudal vertebral centra. Other bones of the skeleton are notably rare in the association, as for example skull bones, forelimb elements and cervical vertebrae, which are represented by few (or no) elements.

Saurischia Seeley, 1887

Sauropoda Marsh, 1878

Titanosauria Bonaparte and Coria, 1993

Indeterminate genus and species

Referred material. MPM-PV-22863, four isolated titanosaurian teeth (Fig 10B-F).

Provenance: These teeth were found within the deposits of the architectural element DF referred as *Magallanodon* Site, and within the architectural element GF referred as the *Isasicursor* II Site (Fig. 3).

Description: All available teeth (Fig.9B-F) are relatively narrow and pencil-like, with high-angled masticatory surfaces, as diagnostic for derived titanosaurs (Calvo, 1994; García and Cerda, 2010). Further, the absence of needle-like teeth and lack of strong enamel ornamentation, argue against rebbachisaurid affinities for the collected specimens (Salgado et al., 2004). However, in spite of its relative homogeneity, two different tooth morphotypes can be recognized among the available materials. A first morphotype includes teeth that are subcircular in cross-section and show smooth tooth enamel (Fig. 9E). A second group of teeth can be distinguished because they are slighlty labiolingual compressed, with gentle mesial and distal carinae and showing some rugosities on enamel surface (Fig. 9F).

730 *Remarks*: Because no teeth are known from the only named titanosaur from the Chorrillo
731 Formation (i.e., *Nullotitan glaciaris*; Novas et al., 2019), none of them can be referred to any
732 previously known species with certainty.

733

734 Theropoda Marsh, 1881

735 Coelurosauria Huene, 1914

736 Megaraptora Benson et al., 2010

737 Megaraptoridae Novas et al., 2013

738 Indeterminate genus and species

739 **Referred material:** MPM-PV-22864, four incomplete and isolated teeth; MPM-PV-22865,
740 nine isolated teeth (Fig. 9 G-I).

741 *Provenance:* Thirteen isolated and fragmentary maxillary and dentary teeth were found, four of
742 them in the *Isasicursor* Site I (MPM-PV-22864; Fig. 3), and other nine elements approximately
743 50 meters below level of the same site (MPM-PV-22865; Fig. 3).

744 *Description*: The size of the teeth is variable. Most of them are represented by crown fragments
745 and only four elements by complete crowns (Fig. 9 G-I). All show an elliptical cross-section
746 with distal and mesial carinae and none can be referred as to premaxillary teeth. As in
747 megaraptorans, the crown is distally curved (Azuma and Currie, 2000; Novas et al., 2008, 2019;
748 Porfiri et al., 2014). The crowns are more lingually than labially curved. The distal margin of
749 the crown shows a sharp carina; which extends all along the apicobasal extension of the crown.
750 The number of denticles on the distal carina is about 2-3 per mm. This value is slightly lower
751 than that observed in other megaraptorans such as *Fukuiraptor, Megaraptor* and *Orkoraptor,* in
752 which 3-4 denticles per mm are present (Azuma and Currie, 2000; Novas et al., 2008; Porfiri et
753 al., 2014). Moreover, MACN-PV 19066 shows 5 denticles per mm (Novas et al., 2019). The

754 denticles are mesiodistally high, apicobasally short and become progressively smaller towards
755 the root. Depending on the specimen, the main axis of the denticles is orthogonally or apically
756 oriented, as reported for other megaraptorans (Azuma and Currie, 2000; Novas et al., 2008;
757 Porfiri et al., 2014). The interdenticular sulci are short and do not extend as blood grooves as
758 occurs in other megaraptorids (e.g., *Australovenator*, *Megaraptor*, *Orkoraptor*, *Murusraptor;*
759 Hocknull et al., 2009; Porfiri et al., 2014; Novas et al., 2008, 2019; Coria and Currie, 2016) but
760 contrasting with the basal megaraptoran *Fukuiraptor* (Azuma and Currie, 2000; Novas et al.,
761 2019). Teeth preserving their tip are devoid of mesial denticles. The teeth are labiolingually
762 much wider mesially than distally. A mesiolingual carina, that is also observed in other
763 megaraptoran specimens (*Fukuiraptor*, *Australovenator*, *Megaraptor*, *Orkoraptor*,
764 *Murusraptor*, MACN-PV 19066), has a weak and distally concave carina that runs along the
765 mesial margin of the lingual side. This mesiolingual carina lacks denticles and is as high as the
766 half of the length of the crown but does not reach the base and tip of the same. Another short
767 carina is observed on the mesial side of the tip of the crown. The tooth crown is almost smooth,
768 lacking enamel wrinkles, as occurs in other megaraptoran taxa (such as A*ustralovenator*,
769 *Orkoraptor*, *Fukuiraptor* and MACN-PV 19066). Wear facets are present on the tip of the
770 crown, and in one of the elements the facet extends almost along a third of the entire height of
771 the crown. The base of the crown is eight-shaped in cross-section as is diagnostic for
772 megaraptorans. However, this constriction is weaker than in other megaraptorans (Novas et al.,
773 2008, 2013; Porfiri et al., 2014; Coria and Currie, 2016) but stronger than in other megaraptoran
774 teeth previously described from the Chorrillo Formation (Novas et al., 2019).

775 *Remarks*: Teeth here described are referred to Megaraptoridae on the basis of the presence of a
776 strongly distally curved crown with the apex placed distally placed from the root, mesial
777 denticles absent or present on the tip of the crown, and presence of 2-3 denticles per mm (Novas
778 et al., 2013; Aranciaga Rolando et al., 2019). The total absence of mesial denticles observed in
779 the teeth from the Chorrillo Formation (MPM-PV-22864-5 and MACN-PV 19066) is observed
780 in other South American megaraptorids, such as *Megaraptor*, *Orkoraptor*, *Murusraptor* and

MACN-PV 19066. By contrast, *Fukuiraptor* shows denticles all along its mesial margin and *Australovenator* (Hocknull et al., 2009), retains denticles on crown tips.

The presence of a mesiolabial carina is absent in the basal megaraptoran *Fukuiraptor* (Azuma and Currie, 2000), but it is present in Megaraptoridae, as it is in *Megaraptor*, *Murusraptor*, *Orkoraptor* and *Australovenator* (Novas et al., 2008, 2019; Hocknull et al., 2009; Benson et al., 2012; Porfiri et al., 2014; Coria and Currie, 2016). However, the isolated tooth from the Strzelecki Group of Australia (Barremian-Aptian strata) shows an intermediate condition between *Fukuiraptor* (Barremian) and more derived megaraporids (Cenomanian-Maastrichtian rocks). In these materials, the mesiolingual carina is more mesially placed, apicobasally higher and shows smooth denticles. This suggests that the mesiolingual carina apparently constitutes a vestige of the mesial carina and that this latter has been reducing through the evolution of Megaraptora.

The Chorrillo Formation has previously provided an isolated tooth referred to Megaraptoridae (Novas et al., 2019). This element differs from MPM-PV-22864-5 on the basis of a higher number of denticles (5 per mm) but shares the presence of a poorly developed eight-shaped constriction. Nevertheless, MACN-PV 19066 comes from old collections made by Bonaparte in the 1980 decade and therefore, its exact stratigraphic position is uncertain. The isolated nature of teeth described for the Chorrillo Formation precludes a determination beyond the family level.

Avialae Gauthier, 1986

Enantiornithes Walker, 1981

Indeterminate genus and species

804 **Referred material**. MPM-PV-22866 the distal fragment of a pedal phalanx (Fig. 16A-D) and
805 two isolated ungual pedal phalanges (MPM-PV-22867; MPM-PV-22868; Fig. 16 E-O).

806 *Provenance:* These remains were found within the deposits of the architectural element FG
807 referred as *Isasicursor* I and *Magallanodon* Sites (Fig. 3).

808 *Description*: The proximal articular surface is dorsoventrally higher than transversely wide,
809 being notably narrower in specimen MPM-PV-22867. Its articular surface is separated into two
810 concave surfaces by a central ridge. The ventral edge of the phalanges is transversely wider than
811 the dorsal edge. The extensor tubercle is short and subtriangular in dorsal view, and in specimen
812 MPM-PV-22868 shows an anterior concavity forming a proximal lip. The flexor tubercle is
813 poorly developed and is teardrop shaped in ventral view, with the apex anteriorly oriented. It is
814 anteriorly delimited by a "V" shaped groove with an anteriorly oriented apex (Fig. 16).

815 *Remarks*: The isolated nature of the phalanges here described, together with some subtle
816 anatomical differences precludes referring them to a single taxon or considering them as
817 belonging to different digits of the same species. Furthermore, the stronger curvature of MPM-
818 PV-22867, may indicate that it belongs to the hallux. Ungual phalanges are referred to
819 enantiornithine birds by virtue of having poorly developed flexor tubercles, a ventral "V"
820 shaped groove delimiting the flexor tubercle and dorsoventrally high and subrectangular-shaped
821 proximal articular surface (Fig. 16; Chiappe, 1993; Chiappe and Calvo, 1994; Kurochkin, 1995;
822 Sanz et al., 2002; Chiappe et al. 2006).

823 Enantiornithine birds have been discovered in different Upper Cretaceous units in northern
824 Patagonian (Chiappe and Calvo, 1994; Schweitzer et al., 2002; Agnolín and Martinelli, 2009;
825 Lawver et al., 2011), but their diversity is notably surpassed by the ornithuromorph birds (e.g.,
826 *Patagopteryx, Alamitornis, Lamarqueavis; Limenavis*; Alvarenga and Bonaparte, 1992; Clarke
827 and Chiappe, 2001; Agnolín et al. 2006; Agnolín and Martinelli, 2009; Agnolín, 2010). *Kookne*
828 *yeutensis* (Novas et al., 2019) is a derived neornithine bird previously reported from the
829 Chorrillo Formation. Agnolín et al., (2017) noted that during the Late Cretaceous,

Enantiornithes were more diverse in continental and equatorial regions, while Ornithuromorpha were taxonomically more diverse in circumpolar areas, but the discovery of enantiornithine remains in the same geological unit (Chorrillo Formation) that yielded *Kookne* indicates a more complex ecological scenario.

7. DISCUSSION

7.1 Depositional Conditions of the Chorrillo Formation

The Chorrillo Formation shows a maximum thickness of ~500 m toward the southwest of the study area, near the international limit between Argentina and Chile, and it decreases considerably toward the east due to the erosional nature of the overlying marine deposits. The exceptional exposures of this succession allowed a detailed description of the architectural elements of the unit. From these descriptions the deposits of the Chorrillo Formation can be divided into channelized units (SS and GS; Fig. 17) and non-channelized units (SL, FG and DF; Fig. 17). Based on the measurement and description of these elements and the interpretation of photopanels it is important to highlight that the Chorrillo Formation is dominated by non-channelized units, especially by fine-grained deposits of the architectural element FG (Figs. 3 and 17). The dominance of fine-grained deposits provides the key to distinguish the Chorrillo Formation from the underlying gravel-dominated La Irene Formation (Macellari et al., 1989; Tettamanti et al., 2018) and the overlying sand-dominated Calafate Formation (Odino-Barreto et al., 2018).

Channelized units are relatively thin in relation with the whole measured thickness and are homogeneously distributed (Figs. 3 and 17). These channels are complex narrow sheets (*sensu* Gibling, 2006) encased within fine-grained floodplain deposits. The presence of mudstone deposits laterally attached to the channelized units (Fig. 18) and the absence of lateral migration elements within the channels, suggest channel abandonment through avulsion mechanism as a common process.

The overall fine-grained dominance of the unit suggests the accumulation in a low-gradient, low net-to-gross and high-accomodation fluvial depositional system (Varela, 2015; Yeste et al., 2020, 2021; Varela et al., 2021). No changes in the fluvial style are interpreted within this unit for two reasons, first because of the constant dominance of fine-grained deposits and second, as no significant erosion surface was recorded in the studied area. The alternation of channelized SS and GS elements was probably related to small fluctuations in the sediment supply/accommodation space ratio (Varela, 2015; Tettamanti et al., 2018).

7.2 Continentalization of the Austral-Magallanes Basin

7.2.1 Paleogeographic implications

The onset of the foreland system of the Austral-Magallanes Basin in the foredeep main depocenter of the basin (Varela et al., 2019), in the Lago Argentino region, is characterized by a thick deep-marine sedimentation that started ~101 ma and includes the evolution from turbiditic to slope deposits (Romans et al., 2011; Malkowski et al., 2017; Daniels et al., 2018; Sickmann et al., 2019). This deep-marine succession was capped on top by a continental expansion of the basin during the Santonian-Campanian (Ghiglione et al., 2021) where deltaic shorelines prograded toward the southeast (Schwartz and Graham, 2015; Schwartz et al., 2017; Moyano-Paz et al., 2018, 2020). The progressive migration of the shoreline toward the southeast produced variations in the distribution of the sedimentary environments triggering the total continentalization of the main depocenter of the Austral-Magallanes Basin at the Lago Argentino region during the latest Campanian-Maastrichtian evidenced by the installation of fluvial systems (Tettamanti et al., 2018; Cuitiño et al., 2019, this study). The sedimentary record of these depositional systems reflects variations between high and low accommodation fluvial systems and does not record the influence of marine processes or transgressions (Tettamanti et al., 2018, this study).

Recent maximum depositional ages from detrital zircons from the underlying La Anita and Cerro Fortaleza formations and from the overlying Calafate Formation (Sickmann et al., 2018,

Ghiglione et al., 2021), in addition to the paleontological content (Novas et al., 2019, this study) suggest an early Maastrichtian age for the Chorrillo Formation. The Maastrichtian deposits of the Chorrillo Formation represent the youngest Cretaceous continental deposits of the foreland stage of the basin in the Lago Argentino region and are bounded on top by the marine transgression of the Calafate Formation (Odino-Barreto et al., 2018).

7.2.2 Paleobiogeographic implications

The development of this 'continental window' that took place during the Late Cretaceous, triggered not only in the development of the fluvial depositional systems but it also provided new ecological niches for colonization by both continental plants, and vertebrates.

Paleobotanical remains reported from the Chorrillo Formation (Novas et al., 2019; this study) do not suggest the same provincialism observed in the vertebrate fauna. Nevertheless, the ongoing study of more megafloristic and palynological assemblages obtained from this unit may provide new sources of evidence for making comparisons with other Patagonian coeval units.

The batrachofauna from the Chorrillo Formation beds sheds some light on anuran diversity and distribution during the Cretaceous in Patagonia. The Mesozoic record of anurans in South America is patchy. Basal anurans of the clade Pipoidea have been recorded from the Early Cretaceous of Brazil (Carvalho et al., 2019) and from mid to Late Cretaceous localities of Brazil and Argentina (Báez, 2000). The record of neobatrachians is also restricted, they being currently represented by nearly complete specimens from the Early and Late Cretaceous of Brazil (e.g., Báez and Perí, 1990; Báez *et al.*, 2009, 2012), and disarticulated specimens from Campanian-Maastrichtian localities in the Chubut and Río Negro provinces of Argentina (i.e., Báez, 1987; Martinelli and Forasiepi, 2004; Muzzopappa and Báez, 2009; Agnolín, 2012). Some incomplete specimens belonging to Calyptocephalellidae were reported from the Dorotea Formation, Chile (Suazo-Lara et al., 2017, 2018).

Fossil calyptocephalellids from the Cretaceous have been assigned to (or related with) the genus *Calyptocephalella* (Báez, 1987; de la Fuente *et al.*, 2007; Agnolín, 2012), the only extant

907 member of Calyptocephalellidae. *Calyptocephalella gayi* is the only living species of this genus,
908 which is endemic to the temperate regions of south-central Chile (Otero *et al.*, 2014). However,
909 in the past, Mesozoic and Cenozoic calyptocephalellids were geographically widespread,
910 including possible reports from Late Cretaceous of India, Africa and Madagascar (Agnolín,
911 2012). Because of their great antiquity, calyptocephalellids were considered as being part of the
912 "ancient assemblage" or "Andean-Antarctic" batrachofaunas that populated the southern end of
913 South America during the Mesozoic, up to Miocene times (Vuilleumier, 1968; Cei, 1980;
914 Agnolín, 2012).

915 In South America, calyptocephalellids are found from Upper Cretaceous to Miocene beds, in
916 several localities along the Patagonia of Argentina and Chile (Agnolín, 2012; Otero et al., 2014,
917 Muzzopapa et al., 2021), whereas reports of other anurans are very scarce and restricted to a few
918 isolated findings (Cione and Baez 2007; Nicoli 2017; Aranciaga-Rolando et al., 2019). Fossil
919 remains from the Eocene and determined as Calyptocephalella were recently reported from
920 Antarctica (Mörs et al., 2020). However the poor preservation of the material, as well as, its
921 particular morphology precludes a clear taxonomic identification.

922 As is the case in most previously known Patagonian localities, anurans from the Chorrillo
923 Formation are represented solely by calyptocephalellids and pipoids. We are not certain if this
924 low diversity reflects the relative isolation of southern Patagonian freshwater basins with
925 respect to the rest of the continent throughout the Cenozoic, and/or a bias in the fossil record. In
926 this regard, it is noteworthy that, in spite of the several climatic changes that occurred during the
927 Cretaceous, Patagonia fossil frogs are mostly represented by two widespread lineages with
928 ancient roots in the continent.

929 Regarding the chelonian record, the chelid-meiolaniiform association described here, the same
930 is also reported from different localities in Patagonia from the Early Cretaceous (e.g., Cerro
931 Barcino Formation) until the mid-Eocene (e.g., Sarmiento Formation), and in Australasia from
932 the mid-Eocene (e.g., Rundle Formation) until the Pleistocene (Gaffney, 1981; Sterli, 2015;
933 Maniel et al., 2016). The chelid-meiolaniform association from the Chorrillo Formation would

represent the southernmost record of this association worldwide. *Yaminuechelys* is a chelid genus known from the Late Cretaceous and Paleocene of Patagonia (La Colonia, Allen, Anacleto, Loncoche, Dorotea, Salamanca, and Roca formations; Maniel et al., 2016). The finding of this genus or a closely related form at the Chorrillo and Dorotea Formations (Novas et al., 2019; Alarcón-Muñoz et al., 2020) demonstrates that this genus was present in the Austral-Magallanes Basin at the end of the Cretaceous and is a key taxon to correlate these two stratigraphic units. It is worth noting that the meiolaniform humerus found in the Chorrillo Formation would represent the southernmost meiolaniform record in South America.

Fossil snakes from Chorrillo Formation previously described (Novas et al., 2019) and the new records reported here include indeterminate ophidians, anilioid and madtsoiids similar to Rionegrophis. This composition is very similar to other snake faunas reported from late Cretaceous Allen and Los Alamitos Formations at Northern Patagonia (Neuquén Basin; Albino, 1987, 1995; Gómez et al., 2008).

The dinosaur fauna of the Chorrillo Formation is diverse, encompassing the colossosaurian titanosaur *Nullotitan glaciaris*, and theropods represented by megaraptorans, unenlagiids and birds. The latter ones include the neornithine *Kookne yeutensis* (Novas et al., 2019) and indeterminate enantiornithines. Furthermore, present findings demonstrate that the Chorrillo Formation has yielded one of the most taxonomically diverse ornithischian faunas from South America, with ankylosaurus, hadrosaurs, and two different kinds of basal euiguanodontians including *Isasicursor santacrucensis* (Novas et al., 2019; Rozadilla et al., 2021, this study). This ornithischian abundance and diversity supports previous claims suggesting that they were far more abundant and diverse in southern Patagonia, Antarctica and Australasia (Novas and Cambiaso, 2004; Novas et al., 2004; Novas, 2009; Agnolín et al., 2010; Rozadilla et al., 2016, 2021) than in northern parts of South America and Africa.

The finding of hadrosaurid and ankylosaurian dinosaurs, pipid and calyptocephalellid frogs, ferugliotheriid gondwanatherians, and chelid turtles related to *Yaminuechelys* constitute a faunistic assemblage that roughly correspond to Maastrichtian faunistic assemblages yielded in

La Colonia Formation (San Jorge Basin, Chubut, central Patagonia; Gasparini et al., 2015), Allen Formation (Neuquén Basin; Leanza et al., 2004; Martinelli and Forasiepi, 2004) and Los Alamitos Formation (Neuquén Basin; Bonaparte et al., 1987). However, as indicated above, the faunistic remains reported so far from the Chorrillo Formation exhibit some differences with northern faunal assemblages, namely, a notable diversification and abundance of ornithischians (particularly elasmarians) and relative abundance of megaraptorans, which is in contrast with northern Patagonia (Novas et al., 2013). This is consistent with previous ideas suggesting some kind of biotic provincialism in Patagonia during the latest Cretaceous times.

Paleobotanical remains reported from the Chorrillo Formation are yet scarce, and do not mirror the provincialism described above for the vertebrate fauna. Nevertheless, new discoveries of megafloristic remains and collecting of palynological assemblages is required to know better the composition and diversity of paleofloristic elements from this sedimentary unit.

7.3 Stratigraphic correlation and comparison with the Dorotea Formation

The lithostratigraphic units that crop out in the Argentinian and Chilean sectors of the basin are named differently (Cuitiño et al., 2019). This issue commonly favored local interpretations for these units, and considerably restricted comparisons between the stratigraphic successions that crop out in both regions. Despite the different names, the successions reflect the same stratigraphic evolution, and some considerations can be made in order to unify evolutionary criteria for the Alta Vista-La Anita-UCCD-Calafate (Argentina) and the Tres Pasos-Dorotea (Chile) successions. It should be noted that the following comparison has no sequence stratigraphic implications.

The Dorotea Formation is a shallowing upward, sandstone dominated unit (Romans et al., 2011; Schwartz and Graham, 2015, Schwarzt et al., 2017) that crops out southern of the study area, in the Magallanes sector of the basin (Chile). It vertically grades from the slope deposits of the Tres Pasos Formation and is overlain by the Man Aike Formation deposits (Romans et al., 2011, Schwarzt and Graham, 2015; Schwartz et al., 2017; Manríquez et al., 2019; George et al., 2020).

The lowermost interval of the Dorotea Formation reflects deposition in a tidal influenced delta front environment that vertically grades into delta plain deposits (Schwartz and Graham, 2015; Schwartz et al., 2017). Recently, Manríquez et al. (2019) presented a stratigraphic analysis for these deposits, dividing the Dorotea Formation and the underlying and overlying units into 6 depositional sequences. In these sequences, the paleontological content is mentioned, proving key elements that allowed a comparison with the stratigraphic succession outcropping in Argentina (Fig. 18).

A prograding fine-grained, large-scale, slope depositional system is recorded in both sectors and is known as the Alta Vista Formation in Argentina and Tres Pasos Formation in Chile (Fig. 18; Romans et al., 2011; Malkowski et al., 2017; Daniels et al., 2018). The slope system deposits are covered by sandstone-dominated, deltaic-coastal deposits of the La Anita Formation in Argentina (Moyano-Paz et al., 2018, 2020) which are correlated with the lowermost interval of the Dorotea Formation (Schwartz and Graham, 2015; Schwartz et al., 2017; Manríquez et al., 2019). The La Anita and Dorotea formations set the end of the deep-marine sedimentation in both regions and the beginning of the continentalization event (Fig. 18; Ghiglione et al., press). These deltaic deposits are covered in theArgentinian region by the UCCD, including the deposits of the Cerro Fortaleza, La Irene and Chorrillo formations. In Chile, there are no lithostratigraphic units associated with continental deposits. However, the medial and upper intervals of the Dorotea Formation, referred as depositional sequences 3, 4 and the lowermost section of sequence 5 (*sensu* Manríquez et al. 2019), are interpreted as a delta plain environment (Schwartz and Graham, 2015), or as fluvial deposits with marine influence (Manríquez et al., 2019).

The vertebrate paleontological content of the Dorotea Formation includes, frogs, turtles, sauropods, theropods, and ornithischians, birds, and mammals (Soto-Acuña et al., 2014; Manriquez et al., 2019; Alarcón-Muñoz et al., 2020; Goin et al., 2020; Martinelli et al., 2021). This faunistic association is very similar to that present at the Chorrillo Formation (Novas et al., 2019; Chimento et al., 2020, 2021; Rozadilla et al., 2021, this study). Further, some taxa, such

as the *Magallanodon* and Hydromedusinae are shared by both formations, and reinforce a biotic correlation between both stratigraphic units. The presence of similar leaf fossils, in particular the Morphotype 1 here presented, which seems closely comparable with the one illustrated by Ortuya et al. (2016) as *Coccoloba?* sp. for the Dorotea Formation may also support this correlation hypothesis. Although sequence stratigraphic analyses are needed, these intervals of the Dorotea Formation could be associated with the Chorrillo Formation representing more distal areas of accumulation in a subaerial part of a deltaic depositional system feed by the fluvial system of the Chorrillo Formation. The uppermost interval of the Dorotea Formation (depositional sequence 5) presents mosasaur and plesiosaur remains (Otero et al., 2015; Manríquez et al., 2019). These levels carrying marine fossils should be correlated with the marine Calafate Formation where a diverse shark fauna is known (Bogan et al., 2016, 2017; D'Angelo et al., 2016; Fig. 19.).

8. CONCLUSIONS

The stratigraphic record of the Chorrillo Formation has been divided into five different architectural elements representing channelized and non-channelized units. Channelized units are characterized by Complex sandy narrow sheet channels (SS) and Complex gravelly narrow sheet channel (GS) elements, and non-channelized units by Sandstone lobes (SL), Thick fine-grained deposits (FG) and Thin dark fine-grained deposits (DF). The overall fine-grained dominance of the succession is interpreted as due to deposition in a low-gradient, low net-to-gross and high-accommodation fluvial depositional system. These fine-grained, fossil-rich, fluvial deposits are part of the UCCD proposed by Tettamanti et al. (2018) and are the youngest continental deposits that accumulated during the Cretaceous in the Lago Argentino region.

The vertebrate fossils yielded by the Chorrillo Formation show clear similarities with roughly coeval beds from northern Patagonia. However, in contrast with Late Cretaceous faunas from Brazil and northern Patagonia, the one from the Chorrillo Formation beds is notable for its diversity in ornithischians and abundance of megaraptorans, a situation more similar to other southern landmasses, including Antarctica and Australasia. Furthermore, the vertebrate

association of Chorrillo Formation matches that reported at the Dorotea Formation of Southern Chile (e.g., hadrosaurs, titanosaurs, gondwanatherians as *Magallanodon*, Hydromedusinae turtles). These similarities, together with sedimentological evidence suggest that these units are equivalent and that they were roughly coeval in age.

ACKNOWLEDGMENTS

The present paper is the result of a joint Argentine-Japanese exploration, carried out in March 2020. The authors would like to thank other members of the crew, including C. Sakata, C. Miyamae, H. Kamei, F. Brissón-Egli, A. Moreno, G. Lio, S. Miner, G. Muñoz, J. De Pasqua, C. Thompson, D. Piazza, G. Lo Coco, A. Misantone, and G. Stoll. A special thanks to Dr. Y. Harashi, former General Director of the National Museum of Nature and Science, Japan. F. Echeverría and D. Fraser from Anita Farm for the hospitality and their valuable geographic knowledge of these territories, and to Coleman Burke for his continuous support in developing dinosaur research in Patagonia. We also acknowledge financial support provided by the Agencia Nacional de Promoción Científica y Técnica (ANPCyT), PICT 2018-01390 to FLA and CONICET. Thanks to Oscar Canto and Carla Almazán (Secretaría de Cultura) for supporting our projects and explorations in Santa Cruz. Authors would like to thank Editor-in-Chief E. Koutsoukos and reviewers A. Martinelli and M.C. Ghiglione for their constructive comments which significantly improved the quality of the manuscript.

REFERENCES

Agnolín, F.L., Novas, F.E., Lio, G.L., 2006. Neornithine bird coracoid from the Upper Cretaceous of Patagonia. Ameghiniana 43(1), 245-248.

Agnolín, F.L., Martinelli, A.G., 2009. Fossil birds from the Late Cretaceous Los Alamitos Formation, Río Negro Province, Argentina. Journal of South American Earth Sciences 27(1), 42-49.

1066 Agnolín, F.L., 2010. An avian coracoid from the Upper Cretaceous of Patagonia, Argentina.
1067 Studia Geologica Salmanticensia 46(2), 99-120.

1068 Agnolín, F.A., 2012. A new Calyptocephalellidae (Anura, Neobatrachia) from the Upper
1069 Cretaceous of Patagonia, Argentina, with comments on its systematic position. Studia
1070 Geologica Salmanticensia 48, 129-178.

1071 Agnolín, F.L., Egli, F.B., Chatterjee, S., García-Marsà, J.A., Novas, F.E., 2017. Vegaviidae, a
1072 new clade of southern diving birds that survived the K/T boundary. The Science of Nature
1073 104(11), 1-9.

1074 Alarcón-Muñoz, J., Soto-Acuña, S., Manríquez, L.M., Fernández, R.A., Bajor, D., Guevara,
1075 J.P., Suazo-Lara, F., Leppe, M., Vargas, A.O., 2020. Freshwater turtles (Testudines: Pleurodira)
1076 in the Upper Cretaceous of Chilean Patagonia. Journal of South American Earth Sciences 102,
1077 102652.

1078 Albino, A.M., 1987. Un nuevo Boidae (Reptilia: Serpentes) del Eoceno temprano de la
1079 Provincia del Chubut, Argentina. Ameghiniana 24, 61-66.

1080 Albino, A.M., 1995. Una nueva serpiente (Reptilia) en el Cretácico Superior de Patagonia,
1081 Argentina. Pesquisas 21, 58-63

1082 Alvarenga, H., Bonaparte, J.F., 1992. A new flightless land bird from the Cretaceous of
1083 Patagonia. Natural History Museum of Los Angeles County Science Series 36, 51-64.

1084 Aranciaga-Rolando, A.M. Agnolín, F. L., Corsolini, J., 2019. A new pipoid frog (Anura,
1085 Pipimorpha) from the Paleogene of Patagonia. Paleobiogeographical implications. Comptes
1086 Rendus Palevol 18(7), 725-734.

1087 Arbe, H.A., 1989. Estratigrafía, discontinuidades y evolución sedimentaria del Cretácico en la
1088 Cuenca Austral, Prov. de Santa Cruz. In: In: Chebli, G., Spalletti, L.A. (Eds.), Cuencas
1089 Sedimentarias Argentinas. Serie de Correlación Geológica 6, 419-442.

1090 Auchter, N.C., Romans, B.W., Hubbard, S.M., Daniels, B.G., Scher, H.D., Buckley, W., 2020.
1091 Intrabasinal sediment recycling from detrital strontium isotope stratigraphy: Geology, v. 48, doi:
1092 10.1130/G47594.1.

1093 Azuma, Y., Currie, P.J., 2000. A new carnosaur (Dinosauria: Theropoda) from the Lower
1094 Cretaceous of Japan. Canadian Journal of Earth Sciences 37, 1735-1753.

1095 Báez, A.M., 1987. Anurans. In: In: Bonaparte, J.F. (Ed.), The Late Cretaceous Fauna de Los
1096 Alamitos, Patagonia, Argentina, vol. 3. Revista del Museo Argentino de Ciencias Naturales
1097 Bernardino Rivadavia, Paleontología, 121-130.

1098 Báez, A. M. 2000. Tertiary anurans from South America. In: H. Heatwole & R.L. Carroll (eds).
1099 Amphibian Biology, Volume 4: Palaeontology, pp. 1388-1401, Surrey Beatty and Sons,
1100 Chipping Norton, Australia.

1101 Báez, A.M., Gasparini, Z., 1977. Orígenes y evolución de los anfibios y reptiles del Cenozoico
1102 de América del Sur. Acta Zoologica Lilloana 14, 149-232.

1103 Báez, A.M., Peri, S., 1990. Revisión de *Wawelia gerholdi*, un anuro del Mioceno de Patagonia.
1104 Ameghiniana 27, 83-94.

1105 Báez, A.M.; Moura, G.J.B., Gómez, R.O., 2009. Anurans from the Lower Cretaceous Crato
1106 Formation of northeastern Brazil: implications for the early divergence of neobatrachians.
1107 Cretaceous Research 30, 829-846.

1108 Báez, A.M., Gómez, R.O., Ribeiro, L.C., Martinelli, A.G., Teixeira, V.P., Ferraz, M. L., 2012.
1109 The diverse cretaceous neobatrachian fauna of South America: *Uberabatrachus carvalhoi*, a
1110 new frog from the Maastrichtian Marília Formation, Minas Gerais, Brazil. Gondwana Research
1111 22(3-4), 1141-1150.

1112 Benson, R.B., Druckenmiller, P.S., 2014. Faunal turnover of marine tetrapods during the
1113 Jurassic–Cretaceous transition. Biological Reviews 89(1), 1-23.

1114 Benson, R.B., Carrano, M.T., Brusatte, S.L., 2010. A new clade of archaic large-bodied
1115 predatory dinosaurs (Theropoda: Allosauroidea) that survived to the latest Mesozoic.
1116 Naturwissenschaften 97, 71.

1117 Berry, E., 1938. Tertiary flora from the río Pichileufu, Argentina. Geological Society of
1118 America, Special Papers, 12, 149 p.

1119 Biddle, K., Uliana, M., Mitchum Jr., R., Fitzgerald, M., Wright, R., 1986. The stratigraphic and
1120 structural evolution of central and eastern Magallanes Basin, Southern America. In: Allen, P.,
1121 Homewoods, P. (Eds.), Foreland Basins. International Association of Sedimentologists, Special
1122 Publication 8, 41-61.

1123 Bogan, S., Agnolín, F.L., Novas, F.E., 2016. New selachian records from the Upper Cretaceous
1124 of southern Patagonia: paleobiogeographical implications and the description of a new taxon.
1125 Journal of Vertebrate Paleontology, 36 (3), 1105235

1126 Bogan, S., Agnolín, F.L., Otero, R.A., Egli, F.B., Suárez, M.E., Soto-Acuna, S., Novas, F.E.,
1127 2017. A new species of the genus *Echinorhinus* (Chondrichthyes, Echinorhiniformes) from the
1128 upper cretaceous of southern South America (Argentina-Chile). Cretaceous Research 78, 89-94.

1129 Bonaparte, J.F., Báez, A.M., Cione, A.L., Andreis, R., de Broin, F. 1987. The Late Cretaceous
1130 fauna of Los Alamitos, Patagonia, Argentina. IX: Résumé. Revista del Museo Argentino de
1131 Ciencias Naturales Bernardino Rivadavia e Instituto Nacional de Investigación de las Ciencias
1132 Naturales. Paleontología, 3 (3), 171-178.

1133 Bonaparte, J.F., Coria, R.A., 1993. Un nuevo y gigantesco saurópodo titanosaurio de la
1134 Formación Río (Albiano-Cenomaniano) de la provincia de Neuquén, Argentina. Ameghiniana
1135 30, 271-282

1136 Bonaparte, J.F., 1996. Dinosaurios de América del Sur. Museo Argentino de Ciencias Naturales
1137 "Bernardino Rivadavia", Buenos Aires, Argentina. 2da Edición. 174 pp.

1138 Bonaparte, J.F., 2002. New Dryolestida (Theria) from the Late Cretaceous of Los Alamitos,
1139 Argentina, and paleogeographical comments. Neues Jahrbuch für Geologie und Paläontologie,
1140 Abhandlungen 224(3), 339-371.

1141 Bonaparte, J.F., Coria, R.A., 1993. Un nuevo y gigantesco saurópodo titanosaurio de la
1142 Formación Río (Albiano-Cenomaniano) de la provincia de Neuquén, Argentina. Ameghiniana
1143 30, 271-282.

1144 Bridge, J.S., 1993. Description and interpretation of fluvial deposits: a critical perspective.
1145 Sedimentology 40, 801-810.

1146 Bridge, J.S., Jalfin, G.A., Georgieff, S.M., 2000. Geometry, lithofacies, and spatial distribution
1147 of Cretaceous fluvial sandstone bodies, San Jorge Basin, Argentina: outcrop analog for the
1148 hydrocarbon-bearing Chubut Group. Journal of Sedimentary Research 70(2), 341-359.

1149 Bridge, J.S., 2003. Rivers and Floodplains: Forms, Processes, and Sedimentary Record.
1150 Blackwell, Oxford, 491 pp.

1151 Bristow, C.S., Skelly, R.L., Ethridge, F.G., 1999. Crevasse splays from the rapidly aggrading,
1152 sand bed, braided Niobrara River, Nebraska: effect of base level rise. Sedimentology 46, 1029-
1153 1047.

1154 Broin, F.L., de la Fuente, M.S., 2001. Oldest world Chelidae (Chelonii, Pleurodira), from the
1155 Cretaceous of Patagonia, Argentina Les plus anciens Chelidae (Chelonii, Pleurodira) du monde,
1156 Crétacé de Patagonie, Argentine. Comptes Rendus de l'Académie des Sciences - Series IIA -
1157 Earth and Planetary Science 333 (8), 463-470.

1158 Burns, C.E., Mountney, N.P., Hodgson, D.M., Colombera, L., 2017. Anatomy and dimensions
1159 of fluvial crevasse-splay deposits: examples from the Cretaceous Castlegate sandstone and
1160 Neslen formation, Utah, USA. Sedimentary Geology 351, 21-35.

1161 Calderón, M.F. Hervé, F. Fuentes, J.C. Fosdick, F. Sepúlveda, G. Galaz., 2016. Tectonic
1162 evolution of Paleozoic and Mesozoic Andean metamorphic complexes and the Rocas Verdes
1163 ophiolites in southern Patagonia M. Ghiglione (Ed.), Geodynamic Evolution of the
1164 Southernmost Andes: Connections With the Scotia Arc, Springer, Berlin (2016), pp. 7-36.

1165 Calvo, J.O., 1994. Jaw mechanics in sauropod dinosaurs. Gaia, 10, 183-193.

1166 Calvo, J.O., Porfiri, J.D., Novas. F.E., 2007. Discovery of a new ornithopod dinosaur from the
1167 Portezuelo Formation (Upper Cretaceous), Neuquén, Patagonia, Argentina. Arquivos do Museu
1168 Nacional Rio de Janeiro 65, 471-483.

1169 Cappetta, H., 2012. Chondrichthyes. Mesozoic and Cenozoic Elasmobranchii: teeth. In Schultze
1170 H.-P. (ed.), Handbook of Paleoichthyology, Volume 3E. 512 pp. Verlag Dr. Friedrich Pfeil,
1171 Munich

1172 Carvalho, I.S., Agnolín, F., Aranciaga-Rolando, M.A., Novas, F.E., Xavier-Neto, J., Freitas,
1173 F.I., Andrade, J.A.F.G., 2019. A new genus of pipimorph frog (Anura) from the early
1174 Cretaceous Crato Formation (Aptian) and the evolution of South American tongueless frogs.
1175 Journal of South American Earth Sciences 92, 222-233.

1176 Casamiquela, R.M., 1958. Un anuro gigante del Mioceno de Patagonia. Revista de la
1177 Asociación Geológica Argentina 13(3-4), 171-184.

1178 Casamiquela, R.M., 1963. ¿Sobre un par de Anuros? Del Mioceno de Rio Negro (Patagonia)
1179 *Wawelia gerholdi* n. gen. et sp.(Ceratophrydidae) y *Gigantobatrachus parodii*
1180 (Leptodactylidae). Ameghiniana 3(5), 141-160.

1181 Casamiquela, R.M., 1978. La zona litoral de la transgresión maastrichtense en el norte de la
1182 Patagonia. Aspectos ecológicos. Ameghiniana 15(1-2), 137-148.

1183 Cei, J.M., 1980. Amphibians of Argentina. Universitá degli studi di Firenze 2, 609.

1184 Chiappe, L.M., 1993. Enantiornithine (Aves) tarsometatarsi from the Cretaceous Lecho
1185 Formation of northwestern Argentina. American Museum Novitates 3083, 1-27.

1186 Chiappe, L.M., Calvo, J.O., 1994. *Neuqueronis volans*, a new Late Cretaceous bird
1187 (Enantiornithes: Avisauridae) from Patagonia, Argentina. Journal of Vertebrate Paleontology
1188 14(2), 230-246.

1189 Chiappe, L.M., Dyke, G.J., 2006. The Early Evolutionary history of birds. Journal of the
1190 Paleontological Society of Korea. 22 (1), 133-151.

1191 Chimento, N.R., Agnolín, F.L., Tsuihiji, T., Manabe, M., Novas, F.E., 2020. New record of a
1192 Mesozoic gondwanatherian mammaliaform from Southern Patagonia. The Science of Nature
1193 107(6), 1-7.

1194 Chimento, N.R., Agnolín, F.L., Novas, F.E., Manabe, M., Tsihuiji, M. 2021. New
1195 gondwanatherian (Mammaliaformes) remains from the Chorrillo Formation (Late Cretaceous)
1196 of Southern Patagonia, Argentina. Cretaceous Research 127, 104947..

1197 Cione, A.L., 1987. The Late Cretaceous fauna of los Alamitos, Patagonia, Argentina. II: The
1198 fishes. Revista del Museo Argentino de Ciencias Naturales Bernardino Rivadavia e Instituto
1199 Nacional de Investigación de las Ciencias Naturales. Paleontología 3(3), 111-120.

1200 Cione, A.L., Báez, A.M., 2007. Peces continentales y anfibios cenozoicos de Argentina: los
1201 últimos cincuenta años. Ameghiniana 50.° aniversario, Publicación Especial 11, 195-220.

1202 Clarke, J.A., Chiappe, L.M., 2001. A new carinate bird from the Late Cretaceous of Patagonia
1203 (Argentina). American Museum Novitates 3323, 1-23.

1204 Clemente, P., Pérez-Arlucea, M., 1993. Depositional architecture of the Cuerda del Pozo
1205 Formation, Lower Cretaceous of the extensional Cameon Basin, North-Central, Spain. Journal
1206 of Sedimentary Petrology 63, 437-452.

1207 Cookson, I.C., 1947. Plant microfossils from the lignites of the Kerguelen Archipelago. BANZ
1208 Antarctic Research Expedition, 1929-1931, Reports, Series A, 2, 129-142.

1209 Cope, E.D., 1869. Extinct Batrachia, Reptilia and Aves of North America. Transactions of the
1210 American Philosophical Society 14, 1-252

1211 Coria, R.A., Salgado, L., 1996. A basal Iguanodontia (Ornithopoda - Ornithischia) from the
1212 Late Cretaceous of South America. Journal of Vertebrate Palaeontology 16(3), 445-457.

1213 Coria, R.A., Calvo, J.O., 2002. A new iguanodontian ornithopod from Neuquén Basin,
1214 Patagonia, Argentina. Journal of Vertebrate Paleontology 22(3), 503-509.

1215 Coria, R. A., Currie, P. J., 2016. A new megaraptoran dinosaur (Dinosauria, Theropoda,
1216 Megaraptoridae) from the Late Cretaceous of Patagonia. PLoS One 11(7), e0157973.

1217 Couper, R.A. 1953. Upper Mesozoic and Cainozoic spores and pollen grains from New Zealand
1218 (Vol. 22). Alexander Doweld.

1219 Cruzado-Caballero, P., Gasca, J.M., Filippi, L.S., Cerda, I.A., Garrido, A.C., 2019. A new
1220 ornithopod dinosaur from the Santonian of Northern Patagonia (Rincón de los Sauces,
1221 Argentina). Cretaceous Research 98, 211-229.

1222 Cuitiño J.I., Varela, A.N., Ghiglione, M.C., Richiano, S., Poiré, D.G., 2019. The Austral-
1223 Magallanes Basin (southern Patagonia): a synthesis of its stratigraphy and evolution. Latin
1224 American Journal of Sedimentology and Basin Analysis 26 (2), 155-166.

1225 Cundall, D., Wallach, V., Rossman, D.A., 1993. The systematic relationships of the snake genus
1226 *Anomochilus*. Zoological Journal of the Linnean Society 109(3). 275-299.

1227 D'Angelo, J.S., Novas, F.E., Otero, R.A., Agnolín, F.L. and Isasi, M.P., 2016. Un nuevo
1228 elasmosáurido (Sauropterygia, Plesiosauroidea) del Cretácico Superior de Santa Cruz,
1229 Argentina y sus afinidades morfológicas con algunos no-aristonectinos de Sudamérica y

1230 Antártida. Libro de resúmenes de las 30 Jornadas Argentinas de paleontología de vertebrados,
1231 "Simposio de reptiles marinos mesozoicos" 90.

1232 Dasgupta, S., Ghosh, P., Gierlowski-Kordesch, E.H., 2017. A discontinuous ephemeral stream
1233 transporting mud aggregates in a continental rift basin: the Late Triassic Maleri Formation,
1234 India. Journal of Sedimentary Research 87, 838-865.

1235 Daniels, B.G., Auchter, N.C., Hubbard, S.M., Romans, B.W., Matthews, W.A., Stright, L.,
1236 2018. Timing of deep-water slope evolution constrained by large-n detrital and volcanic ash
1237 zircon geochronology, Cretaceous Magallanes Basin, Chile. Geological Society of America
1238 Bulletin 130 (3-4), 438-454.

1239 de la Fuente, M.S., Salgado, L., Albino, A., Báez, A.M., Bonaparte, J.F., Calvo, J.O., Chiappe,
1240 L.M., Codorniú, L.S., Coria, R.A., Gasparini, Z., González Riga, B.J., Novas, F.E., Pol, D.,
1241 2007. Tetrápodos continentales del Cretácico de la Argentina. Una síntesis actualizada.
1242 Asociación Paleontológica Argentina, Publicación Especial, 11, 137-153.

1243 Dettman, M.E., Jarzen, D.M., 1988. Angiosperm pollen from uppermost Cretaceous strata of
1244 southeastern Australia and the Antarctic Peninsula. Association of Australasian
1245 Palaeontologists, Memoir 5, 217-237.

1246 Ellis, B., Douglas, C.D., Hickey, L.J., Johnson, K.R., Mitchell, J.D., Wilf, P., Wing, S.L., 2009.
1247 Manual of Leaf Architecture. The New York Botanical Garden Press and Cornell University
1248 Press, New York. 190 p.

1249 Estes, R., Reig, O.A. 1973. The early fossil records of frogs: a review of the evidence. In
1250 Evolutionary biology of the anurans: Contemporary Research on Major Problems, 11-63. Vial,
1251 J.L. (Ed.). Columbia: University of Missouri Press.

1252 Everett, K.R., 1983. Histosols. En: L.P. Wilding, N.E. Smeck and G.F. Hall (Eds.), Pedogenesis
1253 and Soil Taxonomy, II. The Soil Orders, Elsevier Science Publishers, 1-53.

1254 Feruglio, E., 1944. Estudios geológicos y glaciologicos en la región del Lago Argentino
1255 (Patagonia). Boletín de la Academia Nacional de Ciencias 37(1-2), 3-255.

1256 Feruglio, E., 1945 Estudios geológicos y glaciológicos en la región del Lago Argentino
1257 (Patagonia). Boletín de la Academia Nacional de Ciencias de Córdoba 37 (1), 3-255.

1258 Feruglio, 1949. Descripción Geológica de la Patagonia. Yacimientos Petrolíferos Fiscales
1259 (YPF), I, II, III.

1260 Fildani, A., Hessler, A.M., 2005, Stratigraphic record across a retroarc basin inversion: Rocas
1261 Verdes– Magallanes Basin, Patagonian Andes: Geological Society of America Bulletin 117:
1262 1596-1614. doi: 10.1130/B25708.1.

1263 Fildani, A., Cope, T.D., Graham, S.A., Wooden, J.L., 2003. Initiation of the Magallanes
1264 Foreland basin: Timing of the southernmost Patagonian andes Orogeny revised by detrital
1265 zircon provenance analysis. Geology 31, 1081-1084.

1266 Friend, P.F. (1978) Distinctive features of some ancient river systems. In: Fluvial
1267 Sedimentology (Ed. Miall, A.D.). Memories of the Canadian Society of Petroleum Geologists 5,
1268 53-542.

1269 Fossa Mancini, E., Feruglio, E., Yussen de Campana, J.C., 1938. Una reunión de geólogos de
1270 Y.P.F. y el problema de la Terminología Estratigráfica. Boletín de Informaciones Petroleras,
1271 Buenos Aires 171, 31-95.

1272 Fosdick, J.C., Romans, B.W., Fildani, A., Bernhardt, A., Calderón, M., Graham, S.A., 2011.
1273 Kinematic evolution of the Patagonian retroarc fold-and-thrust belt and Magallanes foreland
1274 basin, Chile and Argentina, 51°30’S. Geological Society of America Bulletin 123, 1679-1698.

1275 Gaffney, E.S., 1981. A review of the fossil turtles of Australia. American Museum Novitates,
1276 2720.

1277 Gao, K. Q., Wang, Y., 2001. Mesozoic anurans from Liaoning Province, China, and
1278 phylogenetic relationships of archaeobatrachian anuran clades. Journal of Vertebrate
1279 Paleontology 21(3), 460-476.

1280 Garcia, R.A., Cerda, I.A., 2010. Dentition and histology in titanosaurian dinosaur embryos from
1281 Upper Cretaceous of Patagonia, Argentina. Palaeontology 53(2), 335-346.

1282 Gasparini, Z., Sterli, J., Parras, A., O'Gorman, J.P., Salgado, L., Varela, J., Pol, D., 2015. Late
1283 Cretaceous reptilian biota of the La Colonia Formation, central Patagonia, Argentina:
1284 Occurrences, preservation and paleoenvironments. Cretaceous Research 54, 154-168.

1285 Gee, C.T., Taylor, D.W., 2019. An extinct transitional leaf genus of Nymphaeaceae from the
1286 Eocene lake at Messel, Germany: *Nuphaea engelhardtii* Gee et David w. Taylor gen. Et sp.
1287 Nov. International Journal of Plant Sciences 180(7), 724-736.

1288 George, S.W., Davis, S.N., Fernández, R.A., Manríquez, L.M., Leppe, M.A., Horton, B.K.,
1289 Clarke, J.A., 2020. Chronology of deposition and unconformity development across the
1290 Cretaceous–Paleogene boundary, Magallanes-Austral Basin, Patagonian Andes. Journal of
1291 South American Earth Sciences 97, 102237.

1292 Ghiglione, M.C., Likerman, J., Barberón, V., Giambiagi, L.B., Aguirre-Urreta, B., Suarez, F.,
1293 2014. Geodynamic context for deposition of coarse-grained deep-water axial channel systems in
1294 the Patagonian Andes. Basin Research. 26, 726-745.

1295 Ghiglione, M.C., Naipauer, M., Sue, C., Barberón, V., Valencia, V.A., Aguirre-Urreta, B.M.,
1296 Ramos, V.A., 2015. U-Pb zircon ages from the northern Austral basin and their correlation with
1297 the Early Cretaceous exhumation and volcanism of Patagonia. Cretaceous Research 55, 116-
1298 128.

1299 Ghiglione, M.C., Rocha, E., Raggio, M.F., Ramos, M.E., Ronda, G., Moyano-Paz, D., Varela,
1300 A.N., Valencia, V.A., 2021. Santonian-Campanian continentalization in the Austral-Magallanes

basin: regional correlation, sediment sourcing and geodynamic setting. Cretaceous Research 128, 104968.

Gibling, M.R., 2000. Sequence framework for the Upper Carboniferous Sydney Coalfield, Atlantic Canada. AAPG Annual Meeting

Gibling, M.R., 2006. Width and thickness of fluvial channel bodies and valley fills in the geological record: a literature compilation. Journal of Sedimentary Research 76, 731-770.

Goin, F.J., Martinelli, A.G., Soto-Acuña, S., Vieytes, E.C., Trevisan, C., Manríquez, L.M.E., Fernandes, R.A., Pino, J.P., Trevisan, C., Kaluza, J., Reguero, M.A., Leppe, M., Ortiz, H., Rubilar-Rogers, D., Vargas, A.O., 2020. First Mesozoic mammal from Chile: the southernmost record of a late Cretaceous Gondwanatherian. Boletín del Museo Nacional de Historia Natural de Chile 69, 5-31.

Gómez, R.O., Báez, A.M., Rougier, G.W., 2008. An anilioid snake from the Upper Cretaceous of northern Patagonia. Cretaceous Research 29(3), 481-488.

Gomez, R.O., Baez, A.M., Muzzopappa, P., 2011. A new helmeted frog (Anura: Calyptocephalellidae) from an Eocene subtropical lake in northwestern Patagonia, Argentina. Journal of Vertebrate Paleontology 31, 50-59.

Gomez, R.O., 2016. A new pipid frog from the Upper Cretaceous of Patagonia and early evolution of crown-group Pipidae. Cretaceous Research 62, 52-64.

Gower, D.J., Vidal, N., Spinks, J.N., McCarthy, C.J., 2005. The phylogenetic position of Anomochilidae (Reptilia: Serpentes): first evidence from DNA sequences. Journal of Zoological Systematics and Evolutionary Research 43(4), 315-320.

Hocknull, S.A., White, M.A., Tischler, T.R., Cook, A.G., Calleja, N.D., Sloan, T. and Elliott, D.A., 2009. New Mid-Cretaceous (Latest Albian) Dinosaurs from Winton, Queensland, Australia. PLoS ONE 4, e6190.

1325 Hoffstetter, R. and J.-C. Rage., 1977. Le gisement de vertebres miocenes de La Venta
1326 (Colombie) et sa faune de serpents. Annals of Paleontology (Vert.) 63, 161-190.

1327 Holley, J.A., Sterli, J., Basso, N.G., 2020. Dating the origin and diversification of Pan-Chelidae
1328 (Testudines, Pleurodira) under multiple molecular clock approaches. Contributions to Zoology
1329 89, 146-174.

1330 Hubbard, S.M., Fildani, A., Romans, B.W., Covault, J.A., McHargue, T., 2010. High-relief
1331 slope clinoform development: insights from outcrop, Magallanes Basin, Chile. Journal of
1332 Sediment Research 80, 357-375.

1333 Hünicken, M., 1971. Paleophytología Kurtziana III-4. Atlas de la flora fósil de Cerro Guido
1334 (Cretácico Superior), Ultima Esperanza, Chile (especímenes examinados por F. Kurtz).
1335 Ameghiniana 8, 231-250.

1336 Ibiricu, L.M., Martínez, R.D., Luna, M., Casal, G.A., 2014 reappraisal of *Notohypsilophodon*
1337 *comodorensis* (Ornithischia: Ornithopoda) from the Late Cretaceous of Patagonia, Argentina.
1338 Zootaxa 3786(4) 401-422.

1339 Kluge, A.G., 1993. *Aspidites* and the phylogeny of phythonine snakes. Records of the Australia
1340 Museum Supplement 19 1-77.

1341 Kraemer, P.E., Riccardi, A.C., 1997. Estratigrafía de la región comprendida entre los lagos
1342 Argentino y Viedma (49° 40'- 50°10' LS), Provincia de Santa Cruz. Revista de la Asociación
1343 Geológica Argentina 52, 333-360.

1344 Krausel, R., 1924. Beitrage zur Kenntnis der fossilen Flora Sudamerikas. I. Fossile Holzer aus
1345 Patagonien und benachbarten Gebieten. Arkiv for Botanik 19, 11-36.

1346 Kurochkin, E.N., 1995. Synopsis of Mesozoic birds and early evolution of class Aves.
1347 Archaeopteryx 13, 47-66.

1348 Kurtz, F., 1899. Contribuciones a la Paleophytologia Argentina II. Sobre la existencia de una
1349 Dakota-flora en la Patagonia Austro-occidental (Cerro Guido, Gobernación de Santa Cruz.
1350 Revista Museu de La Plata, Secction Paleontologica 10, 43-50.

1351 Lapparent de Broin, F., 2003. Miocene chelonians from southern Namibia. Memoir of the
1352 Geological Survey of Namibia 19, 67-102.

1353 Lawver, D. R., Debee, A. M., Clarke, J. A., & Rougier, G. W., 2011. A new enantiornithine bird
1354 from the Upper Cretaceous La Colonia Formation of Patagonia, Argentina. Annals of Carnegie
1355 Museum 80(1), 35-42.

1356 Leanza, H.A., Apesteguıa, S., Novas, F.E., de la Fuente, M.S., 2004. Cretaceous terrestrial beds
1357 from the Neuquén Basin (Argentina) and their tetrapod assemblages. Cretaceous Research
1358 25(1), 61-87.

1359 Lee, M.S., Scanlon, J.D., 2002. The Cretaceous marine squamate *Mesoleptos* and the origin of
1360 snakes. Bulletin of the Natural History Museum: Zoology Series 68(2), 131-142.

1361 Lobos, V., Leppe, M., Wilberger, T., Abarzua, A., Manríquez, L., Ortuya, M.J., Garrido, S.,
1362 Fernández, R., 2018. Evidencia fósil en Patagonia para el registro más antiguo de *Brachychiton*
1363 (Malvaceae: Sterculioideae). 1° Congreso Chileno de Paleontología, Abstracts 1: 227-231.

1364 Macellari, C.E., Barrio, C.A., Manassero, M.J., 1989. Upper Cretaceous to Paleocene
1365 depositional sequences and sandstone petrography of southwestern Patagonia (Argentina and
1366 Chile). Journal of South American Earth Sciences 2 (3), 223-239.

1367 Malkowski, M. A., Sharman, G. R., Graham, S. A., Fildani, A., 2015. Characterization and
1368 diachronous initiation of coarse clastic deposition in the Magallanes-Austral foreland basin,
1369 Patagonian Andes. Basin Res. 29, 298-326.

1370 Malkowski, M. A., Grove, M., Graham, S.A., 2016. Unzipping the Patagonian Andes—Long-
1371 lived influence of rifting history on foreland basin evolution. Lithosphere 8, 23-28.

1372 Malkowski, M. A., Schwartz, T.M., Sharman, G.R., Sickmann, Z.T., Graham, S.A., 2017.
1373 Stratigraphic and provenance variations in the early evolution of the Magallanes-Austral
1374 foreland basin: implications for the role of longitudinal versus transverse sediment dispersal
1375 during arc-continent collision. Geological Society of America Bulletin 129, 349-371

1376 Maniel, I.J., Marcelo, S., 2016. A review of the fossil record of turtles of the clade Pan-
1377 Chelidae. Bulletin of the Peabody Museum of Natural History 57(2), 191-227.

1378 Manríquez, L.M., Lavina, E.L., Fernández, R. A., Trevisan, C., Leppe, M. A., 2019.
1379 Campanian-Maastrichtian and Eocene stratigraphic architecture, facies analysis, and
1380 paleoenvironmental evolution of the northern Magallanes Basin (Chilean Patagonia). Journal of
1381 South American Earth Sciences 93, 102-118.

1382 Martinelli, A.G., Forasiepi, A.M., 2004. Late Cretaceous vertebrates from Bajo de Santa Rosa
1383 (Allen Formation), Río Negro province, Argentina, with the description of a new sauropod
1384 dinosaur (Titanosauridae). Revista del Museo Argentino de Ciencias Naturales nueva serie 6,
1385 257-305.

1386 Martinelli, A.G., Soto-Acuña, S., Goin, F.J., Kaluza, J., Bostelmann, J.E., Fonseca, P.H.,
1387 Reguero, M.A. Leppe, M., Vargas, A.O., 2021. New cladotherian mammal from southern Chile
1388 and the evolution of mesungulatid meridiolestidans at the dusk of the Mesozoic era. Scientific
1389 Reports 11(1), 1-18.

1390 Martínez, R.D., 1998. *Notohypsilophodon comodorensis* gen. et sp. nov. Un
1391 Hypsilophodontidae (Ornithischia; Ornithopoda) del Cretácico Superior de Chubut, Patagonia
1392 central. Acta Geologica Leopoldensia 46(47), 119-135.

1393 Miall, A. D., 1996. The geology of fluvial deposits: Sedimentary facies, basin analysis and
1394 petroleum geology: Heidelberg, SpringerVerlag Inc., 582.

1395 Miall, A.D., 2006. Reconstructing the architecture and sequence stratigraphy of the preserved
1396 fluvial record as a tool for reservoir development: A reality check. American Association of
1397 Petroleum Geologists, Bulletin 90, 989-1002.

1398 Mörs, T., Reguero, M. & Vasilyan, D., 2020 First fossil frog from Antarctica: implications for
1399 Eocene high latitude climate conditions and Gondwanan cosmopolitanism of Australobatrachia.
1400 Scientific Reports 10, 5051.

1401 Moyano-Paz, D., Tettamanti, C., Varela, A.N., Cereceda, A., Poiré, D.G., 2018. Depositional
1402 processes and stratigraphic evolution of the Campanian deltaic system of La Anita Formation,
1403 Austral-Magallanes Basin, Patagonia, Argentina. Latin American Journal of Sedimentology and
1404 Basin Analysis 25 (2), 69-92.

1405 Moyano-Paz, D., Richiano, S., Varela, A.N., Gómez Dacal, A.R., Poiré, D.G., 2020.
1406 Ichnological signatures from wave- and fluvial-dominated deltas: The La Anita Formation,
1407 Upper Cretaceous, Austral-Magallanes Basin, Patagonia. Marine and Petroleum Geology 114,
1408 104168.

1409 Muzzopappa, P., Báez, A.M., 2009. Systematic status of the mid- Tertiary neobatrachian frog
1410 *Calyptocephalella canqueli* from Patagonia (Argentina), with comments on the evolution of the
1411 genus. Ameghiniana 46 113-125.

1412 Muzzopappa, P., Martinelli, A.G., Garderes, J.P., Rougier, G.W. 2021. Exceptional avian pellet
1413 from the paleocene of Patagonia and description of its content: a new species of
1414 calyptocephalellid (Neobatrachia) anuran. Papers in Palaeontology, 7 (2), 1133-1146.

1415 Natland, M.L., Gonzalez, E., Cation, A., Ernst, M., 1974. A System of Stages for Correlation of
1416 Magallanes Basin Sediments. Geological Society of America, Memoir 139, 126.

1417 Nicoli, L., 2017. The Presence of *Lepidobatrachus* (Anura, Ceratophryidae) in the Neogene of
1418 the La Pampa Province, Argentina. Ameghiniana, 54 (6), 700-705.

1419 Novas, F.E., Cambiaso, A., Ambrosio, A., 2004. A new basal iguanodontian (Dinosauria,
1420 Ornithischia) from the Upper Cretaceous of Patagonia. Ameghiniana 41, 75-82.

1421 Novas, F.E., Ezcurra, M.D. Lecuona, A., 2008. *Orkoraptor burkei* nov.gen. et sp., a large
1422 theropod from the Maastrichtian Pari Aike Formation, Southern Patagonia, Argentina.
1423 Cretaceous Research 29, 468-480.

1424 Novas, F.E., Pol, D., Canale, J.I., Porfiri, J.D., Calvo, J.O., 2009. A bizarre Cretaceous theropod
1425 dinosaur from Patagonia and the evolution of Gondwanan dromaeosaurids. Proceedings of the
1426 Royal Society B: Biological Sciences 276 (1659), 1101-1107.

1427 Novas, F.E., Agnolín, F.L., Ezcurra, M.D., Porfiri, J. and Canale, J.I. 2013. Evolution of the
1428 carnivorous dinosaurs during the Cretaceous: the evidence from Patagonia. Cretaceous Research
1429 45, 174-215.

1430 Novas, F.E., Agnolín, F.L., Rozadilla, S., Aranciaga-Rolando, AM.., Brissón-Eli, F., Motta,
1431 M.J., Cerroni, M.A., Ezcurra, M.D., Martinelli, A.G., D'Angelo, J.S., Alvarez-Herrera, G.P.,
1432 Gentil, A.R., Bogan. S., Chimento, N.R., García-marsà, J.A., Lo Coco, G.E., Miquel, S.E.,
1433 Brito, F.F., Vera, E.I., Perez-Loinase, V.S., Fernandez, V., Salgado, L., 2019. Paleontological
1434 discoveries in the Chorrillo Formation (upper Campanian-lower Maastrichtian, Upper
1435 Cretaceous), Santa Cruz Province, Patagonia, Argentina. Revista del Museo Argentino de
1436 Ciencias Naturales nueva serie 21 (2), 217-293.

1437 Odino-Barreto, A.L., Cereceda, A., Gómez-Peral, L.E., Coronel, M.D., Tettamanti, C., Poiré,
1438 D.G., 2018. Sedimentology of the shallow marine deposits of the Calafate formation during the
1439 maastrichtian transgression at Lago Argentino, austral Magallanes Basin, Argentina. Latin
1440 American Journal of Sedimentology and Basin Analysis 25 (2), 169-191.

1441 O'Gorman, J.P. 2016. A small body sized non-aristonectine elasmosaurid (Sauropterygia,
1442 Plesiosauria) from the Late Cretaceous of Patagonia with comments on the relationships of the
1443 Patagonian and Antarctic elasmosaurids. Ameghiniana 53(3), 245-268.

1444 O'Gorman, J.P., 2020. Elasmosaurid phylogeny and paleobiogeography, with a reappraisal of
1445 *Aphrosaurus furlongi* from the Maastrichtian of the Moreno Formation. Journal of Vertebrate
1446 Paleontology, 39(5), e1692025.

1447 Ortiz-Jaureguizar, E., Cladera, G.A., 2006. Paleoenvironmental evolution of southern South
1448 America during the Cenozoic. Journal of Arid Environments 66(3), 498-532.

1449 Ortuya, M.J., Leppe, M., Pineda, M.V., 2016. Nuevos antecedentes estratigráficos y
1450 paleontológicos de la cuenca cretácica de Magallanes, extremo austral de Chile. V Simpósio de
1451 Paleontologia do Chile, Libro de resúmenes, p. 143.

1452 Otero, R.A., Jimenez-Huidobro, P., Soto-Acuna, S., Yury-Yánez, R.E., 2014. Evidence of a
1453 giant helmeted frog (Australobatrachia, Calyptocephalellidae) from Eocene levels of the
1454 Magallanes Basin, southernmost Chile. Journal of South American Earth Sciences 55, 133-140.

1455 Otero, R.A., Soto-Acuña, S., Salazar, C., Oyarzún, J.L., 2015. New elasmosaurids
1456 (Sauropterygia, Plesiosauria) from the Late Cretaceous of the Magallanes Basin, Chilean
1457 Patagonia: evidence of a faunal turnover during the Maastrichtian along the Weddellian
1458 Biogeographic Province. Andean Geology 42(2), 237-267.

1459 Owen, R., 1860. On the orders of fossil and Recent Reptilia, and their distribution in time.
1460 Report of the British Association for the Advancement of Science 29, 153-166.

1461 Owen, G., Santos, M.G., 2014. Soft-sediment deformation in a pre-vegetation river system: the
1462 Neoproterozoic Torridonian of NWScotland. Proceedings of the Geologists' Association., 125,
1463 511-523.

1464 Pankhurst, R.J., Riley, T.R., Fanning, C.M., Kelley, S.P., 2000. Episodic silicic Volcanism in
1465 Patagonia and Antarctic Peninsula: Chronology of magmatism associated with the break-up of
1466 Gondwana. Journal of Petrology 41, 605-625.

1467 Poiré, D.G., Iglesias, A., Varela, A.N., Richiano, S., Mejía Ibañez, M., Stroemberg, C., 2017.
1468 Edades U-Pb en zircones de tobas de la Fm. Piedra Clavada, pcia. de Santa Cruz, Argentina: un
1469 marcador albiano tardío para la evolución tectónica y biológica de la Cuenca Austral. In: Actas
1470 del XX Congreso Geológico Argentino TU-S15, 95-98.

1471 Porfiri, J.D., Novas, F.E., Calvo, J.O., Agnolín, F.L., Ezcurra, M.D., Cerda, I.A., 2014. Juvenile
1472 specimen of *Megaraptor* (Dinosauria, Theropoda) sheds light about tyrannosauroid radiation.
1473 Cretaceous Research 51, 35-55.

1474 Powell, J.E., 2003. Revision of South American titanosaurid dinosaurs: palaeobiological,
1475 palaeobio-geographical and phylogenetic aspects. Records of the Queen Victoria Museum 111,
1476 1-173.

1477 Rage J., 1984, Encyclopedia of Paleoherpetology. Part 11. Serpentes, Stuttgart - New York.

1478 Rage, J.C., 1998. Fossil snakes from the Palaeocene of São José de Itaboraí, Brazil. Part I.
1479 Madtsoiidae, Aniliidae. Palaeovertebrata 27(3-4), 109-144.

1480 Reig, O.A., 1958. Proposiciones para una nueva macrosistematica de los anuros (Nota
1481 preliminar). Physis 26, 109-118.

1482 Reig, O.A., 1960. Las relaciones genéricas del anuro chileno *Calyptocephalella gayi* (Dum. &
1483 Bibr.). Actas y Trabajos del Primer Congreso Sudamericano de Zoología 4, 113-131.

1484 Retallack, G.J., 2001. A 300-million-year record of atmospheric carbon dioxide from fossil
1485 plant cuticles. Nature 411, 287-290.

1486 Richiano, S., Varela, A.N., Cereceda, A., Poiré, D.G., 2012. Evolución paleoambiental de la
1487 Formación Río Mayer, cretácico inferior, cuenca austral, Patagonia Argentina. Latin American
1488 Journal of Sedimentology and Basin Analysis 19, 3-26.

1489 Richiano, S., Poiré, D.G., Varela, A.N., 2013. Icnología de la Formación Río Mayer, Cretácico
1490 Inferior, SO Gondwana, Patagonia, Argentina. Ameghiniana 50, 273-286.

1491 Richiano, S., Varela, A.N., Gómez-Peral, L.E., Cereceda, A., Poiré, D.G., 2015. Composition of
1492 the lower cretaceous black shales from the Austral basin (Patagonia, Argentina): implication for
1493 unconventional reservoirs in the southern Andes. Marine and Petroleum Geology 66, 764-790.

1494 Rieppel, O., 1988. A review of the origin of snakes. Evolutionary biology: 37-130.

1495 Rivera, H.A., Le Roux, J.P., Farías, M., Gutiérrez, N.M., Sanchez, A., Palma-Heldt, S., 2020.
1496 Tectonic controls on the maastrichtian-danian transgression in the magallanes-austral foreland
1497 basin (Chile): implications for the growth of the southern patagonian Andes. Sedimentary
1498 Geology 403, 105645.

1499 Rocek, 2013. Mesozoic and Tertiary Anura of Laurasia. Palaeobiodiversity and
1500 Palaeoenvironments 93, 397-439

1501 Rodríguez, J.F., Miller, M., 2005. Cuenca Austral. In: Frontera Exploratoria de la Argentina.
1502 Chebli, G.A., Cortiñas, J.S., Spalletti, L.A., Legarreta, L., Vallejo, E.L., (Eds.). Congreso de
1503 exploración y Desarrollo de Hidrocarburos, No. 6, Actas 15, 307-323. Mar del Plata.

1504 Romans, B.W., Hubbard, S.M., Graham, S.A., 2009. Stratigraphic evolution of an outcropping
1505 continental slope system, Tres Pasos formation at Cerro Divisadero, Chile. Sedimentology 56,
1506 737-764.

1507 Romans, B.W., Fildani, A., Hubbard, S.M., Covault, J.A., Fosdick, J.C., Graham, S.A., 2011.
1508 Evolution of deep-water stratigraphic architecture, Magallanes Basin, Chile. Marine and
1509 Petroleum Geology 28 (3), 612-628.

1510 Rossetti, D.F., Santos, A.E., 2003. Events of sediment deformation and mass failure in Upper
1511 Cretaceous estuarine deposits (Cameta´ Basin, northern Brazil) as evidence for seismic activity.
1512 Sedimentary Geology 161, 107-130.

1513 Rozadilla, S., Agnolín, F.L., Novas, FE., Aranciaga-Rolando, A.M., Motta, M.J., Lirio, J.M.,
1514 Isasi, M.P., 2016. A new ornithopod (Dinosauria, Ornithischia) from the Upper Cretaceous of
1515 Antarctica and its palaeobiogeographical implicances. Cretaceous Research 57, 311-324.

1516 Rozadilla, S., Agnolín, F.L., Novas, F.E., 2019. Osteology of the Patagonian ornithopod
1517 *Talenkauen santacrucencis* (Dinosauria, Ornithischia). Journal of Systematic Palaeontology 17
1518 (24), 2043-2089.

1519 Rozadilla, S., Agnolín, F.L, Manabe, M., Tsuihiji, T., Novas, F.E., 2021. Ornithischian Remains
1520 from the Chorrillo Formation (Upper Cretaceous) of Southern Patagonia, Argentina, and their
1521 Implications on Ornithischian Paleogeography in the Southern Hemisphere. Cretaceous
1522 Research 125, 104881.

1523 Salgado, L., Garrido, A., Cocca, S.E., Cocca., J.R., 2004. Lower Cretaceous rebbachisaurid
1524 sauropods from Cerro Aguada del León (Lohan Cura Formation), Neuquén Province,
1525 northwestern Patagonia, Argentina. Journal of Vertebrate Paleontology 24 (4), 903-912.

1526 Santamarina P.E., Barreda, V.D., Moyano-Paz, D., Tettamanti, C., Iglesias, A., Poiré, D.G.,
1527 Varela, A.N., 2020. Palynoflora from the La Anita Formation (Maastrichtian), Austral-
1528 Magallanes Basin, Argentina. Revista del Museo Argentino de Ciencias Naturales nueva serie
1529 21 (1), 47-56.

1530 Sanz, J. L., Pérez-Moreno, B.P., Chiappe, L.M., Buscalioni, A.D., 2002. The birds from the
1531 lower Cretaceous of las hoyas (Province of Cuenca, Spain). Mesozoic birds: above the heads of
1532 dinosaurs, 209-229.

1533 Scanlon, J.D., Lee, M.S., 2002. Varanoid-like dentition in primitive snakes (Madtsoiidae).
1534 Journal of Herpetology, 100-106.

1535 Schroeter, E.R., Egerton, V.M., Ibiricu, L.M., Lacovara, K.J. 2014. Lamniform Shark Teeth
1536 from the Late Cretaceous of Southernmost South America (Santa Cruz Province, Argentina).
1537 Plos one 9 (8), e104800.

1538 Schuster, T.M., Setaro, S.D., Kron, K.A., 2013. Age estimates for the buckwheat Family
1539 Polygonaceae based on sequence data calibrated by fossils and with a focus on the Amphi-
1540 Pacific Muehlenbeckia. PLoS ONE 8, e61261. https://doi.org/10.1371/journal.pone.0061261.

1541 Schwartz, T.M., Graham, S.A., 2015. Stratigraphic architecture of a tide- influenced
1542 shelf- edge delta, upper cretaceous Dorotea Formation, Magallanes- Austral basin, Patagonia.
1543 Sedimentology 62 (4), 1039-1077.

1544 Schwartz, T.M., Fosdick, J.C., Graham, S.A., 2017. Using detrital zircon U- Pb ages to
1545 calculate Late Cretaceous sedimentation rates in the Magallanes- Austral basin, Patagonia.
1546 Basin Research 29 (6), 725-746.

1547 Schweitzer, M.H., Jackson, F.D., Chiappe, L.M., Schmitt, J.G., Calvo, J.O., Rubilar-Rogers,
1548 D.E., 2002. Late Cretaceous avian eggs with embryos from Argentina. Journal of Vertebrate
1549 Paleontology 22 (1), 191-195.

1550 Sickmann, Z.T., Schwartz, T.M., Graham, S.A., 2018. Refining stratigraphy and tectonic history
1551 using detrital zircón máximum depositional age: an example from the Cerro Fortaleza
1552 Formation, Austral Basin, southern Patagonia. Basin Research 30(4), 708-729.
1553 https://doi.org/10.1111/bre.12272.

1554 Sickmann, Z.T., Schwartz, T.M., Malkowski, M.A., Dobbs, S.C., Graham, S.A., 2019.
1555 Interpreting large detrital geochronology data sets in retroarc foreland basins: An example from
1556 the Magallanes-Austral Basin, southernmost Patagonia. Lithosphere.
1557 https://doi.org/10.1130/L1060.1

1558 Smith, N.D., Cross, T.A., Dufficy, J.P., Clough, S.R., 1989. Anatomy of an avulsion.
1559 Sedimentology 36, 1-23.

1560 Soto-Acuña, S. Jujihara, T., Novas, F.E., Leppe, M, González, E., Stinnesbeck, W., Isasi, M.P.,
1561 Rubilar-Rogers, D., Vargas, A.O., 2014. Hadrosaurios (Ornithopoda: Hadrosauridae) en el

1562 Cretácico Superior del extremo austral de América del Sur. IV Simposio Paleontología en Chile,
1563 Universidad Austral de Chile Resúmenes, 73.

1564 Sterli, J., 2015. A review of the fossil record of Gondwanan turtles of the clade Meiolaniformes.
1565 Bulletin of the Peabody Museum of Natural History 56 (1), 21-45.

1566 Sterli, J., De la Fuente, M.S., 2019. Cranial and post-cranial remains and phylogenetic
1567 relationships of the Gondwanan meiolaniform turtle *Peligrochelys walshae* from the Paleocene
1568 of Chubut, Argentina. Journal of Paleontology 93, 798-821.

1569 Suazo-Lara, F., Fernández-Jiménez, R., Soto-Acuña, S., Manríquez, L., Alarcón-Muñoz, J.,
1570 Aravena, B., Vargas, A.O., Leppe, M., 2017. Primer registro de Calyptocephalellidae (Anura,
1571 Australobatrachia) en el Cretácico Superior de Chile. I Reunión de Paleontología de
1572 Vertebrados de Chile, Santiago.

1573 Suazo Lara, F., Alarcón-Muñoz, J., Fernández-Jiménez, R., Kaluza, J., Manríquez, L., Milla, V.,
1574 Soto-Acuña, S., Leppe, M., 2018. Nuevos registros de anuros del Valle del Río de Las Chinas
1575 (Formación Dorotea, Cretácico Superior), Región de Magallanes, Chile. I Congreso Chileno de
1576 Paleontología, Punta Arenas – Puerto Natales.

1577 Taylor, D.W., Gee, C.T., 2014. Phylogenetic analysis of fossil water lilies based on leaf
1578 architecture and vegetative characters: testing phylogenetic hypotheses from molecular studies.
1579 Bulletin of the Peabody Museum of Natural History 55, 89-110.

1580 Tettamanti, C., Moyano-Paz, D., Varela, A.N., Tineo, D.E., Gómez-Peral, L.E., Poiré, D.G.,
1581 Cereceda, A., Odino Barreto, A.L., 2018. Sedimentology and fluvial styles of the Uppermost
1582 Cretaceous Continental Deposits of the Austral-Magallanes Basin, Patagonia, Argentina. Latin
1583 American Journal of Sedimentology and Basin Analysis 25 (2), 149-168.

1584 Tchernov, E., Rieppel, O., Zaher, H., Polcyn, M.J., Jacobs, L.L., 2000. A fossil snake with
1585 limbs. Science 287 (5460), 2010-2012.

1586 Varela, A.N., 2015. Tectonic control of accommodation space and sediment supply within the
1587 Mata Amarilla Formation (lower Upper Cretaceous) Patagonia, Argentina. Sedimentology 62
1588 (3), 867-896.

1589 Varela, A.N., Poiré, D.G., Martin, T., Gerdes, A., Goin, F.J., Gelfo, J.N., Hoffmann, S., 2012.
1590 U-Pb zircon constraints on the age of the Cretaceous Mata Amarilla Formation, Southern
1591 Patagonia, Argentina: its relationship with the evolution of the Austral Basin. Andean Geology
1592 39 (3), 359-379.

1593 Varela, A.N., Veiga, G.D., Poiré, D.G., 2012b. Sequence stratigraphic analysis of Cenomanian
1594 greenhouse palaeosols: A case study from southern Patagonia, Argentina. Sedimentary Geology
1595 271, 67-82.

1596 Varela, A.N., Richiano, S., D'Elia, L., Moyano-Paz, D., Tettamanti, C., Poiré, D.G., 2019.
1597 Sedimentology and stratigraphy of the Puesto El Moro Formation, Patagonia, Argentina:
1598 Implications for upper cretaceous paleogeographic reconstruction and compartmentalization of
1599 the Austral-Magallanes Basin. Journal of South American Earth Science 92, 466-480.

1600 Varela, A.N., Yeste, L.M., Viseras, C., García-García, F., Moyano-Paz, D., 2021. Implications
1601 of palaeosols in low net-to-gross fluvial architecture reconstruction: Reservoir analogues from
1602 Patagonia and Spain. Palaeogeography, Palaeoclimatology, Palaeoecology577, 110553..

1603 Veiga, G.D., Spalletti, L.A. and Flint, S.S., 2007. Anatomy of a fluvial lowstand wedge: the
1604 Avile Member of the Agrio Formation (Hauterivian) in central Neuquén Basin (northwest
1605 Neuquen province), Argentina. In: Sedimentary Environments, Processes and Basins. A Tribute
1606 to Peter Friend (Eds Nichols, G., Williams, E. and Paola, C.), International Association of
1607 Sedimentologists, Special Publication 38, 341-365.

1608 Vidal, N., Hedges, S.B., 2002. Higher-level relationships of caenophidian snakes inferred from
1609 four nuclear and mitochondrial genes. Comptes Rendus Biologies 325 (9), 987-995.

1610 Vidal, N., Hedges, S.B., 2004. Molecular evidence for a terrestrial origin of snakes. Proceedings
1611 of the Royal Society of London. Series B: Biological Sciences 271 (4), S226-S229.

1612 Vlachos, E., Randolfe, E., Sterli, J., Leardi, J.M., 2018. Changes in the diversity of turtles
1613 (Testudinata) in South America from the Late Triassic to the present. Ameghiniana 55 (6), 619-
1614 643.

1615 Vuilleumier, F., 1968. Origin of frogs of Patagonian forests. Nature 219: 87-89.

1616 Wakelin-King, G.A., Webb, J.A., 2007. Threshold-dominated fluvial styles in an arid-zone
1617 mud-aggregate river: the uplands of Fowlers Creek, Australia. Geomorphology 85, 114-127.

1618 Wilcox, T. P., Zwickl, D. J., Heath, T. A., Hillis, D.M., 2002. Phylogenetic relationships of the
1619 dwarf boas and a comparison of Bayesian and bootstrap measures of phylogenetic support.
1620 Molecular Phylogenetics and Evolution 25 (2), 361-371.

1621 Wilson, T.J. (1991) Transition from back- arc to foreland basin development in the
1622 southernmost Andes: stratigraphic record from the Ultima Esperanza District, Chile. Geological
1623 Society of America 103, 98–111

1624 Worthy, T.H., Tennyson, A.J., Scofield, R.P., Hand, S.J., 2013. Early Miocene fossil frogs
1625 (Anura: Leiopelmatidae) from New Zealand. Journal of the Royal Society of New Zealand 43
1626 (4), 211-230.

1627 Wright, V.P., Marriott, S.B., 2007. The dangers of taking mud for granted: lessons from Lower
1628 Old Red Sandstone dryland river systems of South Wales. Sedimentary Geology 195, 91-100.

1629 Yabe, A., Uemura, K., Nishida, H., Yamada, T., 2006. Geological notes on plant megafossil
1630 localities at Cerro Guido, Ultima Esperanza, Magallanes (XII) Region, Chile. In: Nishida, H.
1631 (Ed.), Post-Cretaceous Floristic Changes in Southern Patagonia, Chile. Chuo University, Tokyo,
1632 pp. 5-10.

Yeste, L.M., Varela, A.N., Viseras, C., McDougall, N.D., García-García, F., 2020. Reservoir architecture and heterogeneity distribution in floodplain sandstones: Key features in outcrop, core and wireline logs. Sedimentology 67, 3355-3388.

TABLE AND FIGURE CAPTION

Table 1. Sedimentary facies identified in the Chorrillo Formation.

Figure 1. A, Location map of the Austral-Magallanes Basin (modified from Moyano-Paz et al., 2020). B, Stratigraphic scheme of the sedimentary infill for the Austral-Magallanes Basin in the Lago Argentino region (modified from Ghighlione et al., 2014; Sickmann et al., 2018; Moyano-Paz et al., 2018; Tettamanti et al., 2018).

Figure 2. Geological map of the study area showing the distribution of the stratigraphic units (modified from Kraemer and Riccardi, 1997; Ghiglione et al., 2014; Moyano-Paz et al., 2018).

Figure 3. Detailed measured section of the Chorrillo Formation showing the main sedimentary features, fossil content distribution and the vertical distribution of the architectural element

Figure 4. A-B, Outcrop photographs of the channel shaped, erosion-based bodies of the architectural element SS. C, Detail of cross-bedded individual storeys bounded by erosion surfaces. D, Detail of storey infill showing trough cross-bedding facies (St). E, Detail of wood impressions toward the base of the channel constituting a basal lag.

Figure 5. A-B, Outcrop photographs of the channel shaped, erosion-based bodies of the architectural element GS.

Figure 6. A-B, Outcrop photographs of the lobate bodies of the architectural element SL. A, Detail of gradual increase in grain size from the fine-grained deposits of FG element. B, Detail of irregular convex-up top.

Figure 7. A, Outcrop photograph of the reddish and greenish massive mudstones intercalated with sandstone beds of the architectural element FG. B, Detail of rhizolith. C, Detail of

slickensides. D, Detail of granular and subangular to angular blocky peds. E, Detail of the organic-rich grey, thin-laminated mudstones of the architectural element DF. F-G, Detail of well preserved plant remains.

Figure 8. A-D, Plant impressions collected from the architectural element FG at 215 m in the stratigraphic column. A, Fragment of leaves probably related to monocots with parallel veins (Morphotype 6), MPM-PB-22809. B, Specimen with a stout midvein (white arrows) and lateral veins diverging that produce several dichotomies at the same level before reaching the margin, MPM-PB-22810. C–D, Specimen without a midven, presenting radiating veins that dichotomize 3-4 times at comparable levels, being the last dichotomies located near the margin and ending in a loop (white arrow), MPM-PB-22811. E–L, Plant impressions collected from the architectural element FG at 295 m in the stratigraphic column. E–G, Specimens of elliptic asymmetric leaves with pinnate primary venation and brochidodromous secondary venation and looped exterior tertiaries (Morphotype 1). E, MPM-PB-22801. F, MPM-PB-22802. G, MPM-PB-22803. H, Leaf that differs from the others recognized morphotypes in having palmate primary venation (Morphotype 2), MPM-PB-22804. I, Specimen of partial leaf which preserves its acute apex and primary vein with decurrent secondaries (Morphotype 3), MPM-PB-22806. J, Specimen with a straight midvein with a pinnate pattern, with non-decurrent secondaries arising in acute angles (Morphotype 4), MPM-PB-22807. K, Fragments of leaves with one-ranked parallel veins (Morphotype 5), MPM-PB-22808. L, Root impressions, MPM-PB-22805. Scale bars: A-D:1 mm, E-L:10 mm.**Figure 9.** A, Indeterminate Lamniform tooth (MPM-PV-22839) in lingual and mesial views; B-F, selected sauropod teeth (MPM-PV-22863) B,D,E, pencil-like morphotype; C,F, thick morphotype; G-I, selected megaraptorid teeth (MPM-PV-22864 and MPM-PV-22865). Abbreviations: k, keel; mc, mesiolabial carina; wf, wear facet. Scale bar: 1 cm.

Figure 10. A-C, distal end of right humerus of an indeterminate pipoid (MPM-PV-22840) in A, anterior; B, posterior; and C, distal views; D-M, *Calyptocephalella* sp.; D,E, incomplete left maxilla (MPM-PV-22841) in D, lateral, and E, medial views; F,G, incomplete right maxilla (MPM-PV-22842) in F, dorsolateral; and G, medial views; H,I, proximal end of right radioulna

(MPM-PV-22844) in H, medial and I, lateral views; J,K, incomplete right ilium (MPM-PV-22843) in J, lateral; and K, medial views; L,M, proximal end of left tibiofibula (MPM-PV-22845) in L anterior; and M, posterior views. Abbreviations. ac, acetabulum; as, articular surface for the humerus; ba, articular ball; coi, concavity for the opposite ilium; cs, concave surface; cu, ventral cubital fossa; dt, dorsal tubercle/crest; fo, foramen; fp, fibular process; le, lateral epicondyle; me, medial epicondyle; ogc, oblique groove and crest; ol, olecranal fossa; ole, olecranon; sab, subacetabular process; sac, supracetabular process; sam, smooth alveolar margin; tp, tibial process; pd, pars dentalis; ps, palatal shelf. Scale bar 5 mm.

Figure 11. A-D, Anilioidea, possible mid-precloacal vertebra (MPM-PV-22847) in A, ventral view; B, lateral view; C, dorsal view; and D, posterior view. E-F, cf. *Rionegrophis* sp., incomplete trunk vertebra (MPM-PV-22848) in E, ventral; and F right lateral views. G-J, Indeterminate elasmosaurid vertebrae; G-H, cervical vertebra (MPM-PV-22859) in G, ventral view; H, anterior view; I-J, dorsal vertebra (MPM-PV-22860) in I, lateral view; J, anterior view. Abbreviations: hk, haemal keel; nc, neural canal; par, parapophyses; po, postzygapophyseal process; scf, subcentral foramina; sd, subcentral depression; sr, subcentral ridge; vn, ventral notch. Scale bar: A-F, 5 mm; G-J, 1 cm.

Figure 12. Selected carapace plates of an indeterminate Hydromedusinae (Chelidae). A,B,E,H,K,M,P,R, external; C, J, ventral; F,I,L,N,Q, visceral; and D,G,O, side views. A–D, left peripheral 3 or 4 (MPM-PV-22849); E, F, bridge peripheral (MPM-PV-22850); G–I indeterminate fragment (MPM-PV-22851); J–L bridge peripheral (MPM-PV-22852); M, N, right hypoplastron (MPM-PV-22853); O, bridge buttress (MPM-PV-22854); P, Q, plastral fragment (MPM-PV-22856); R, ?plastral fragment (MPM-PV-22855). Abbreviations: AB, abdominal scute; FE, femoral scute; MA, marginal scute; PL, pleural scute; scar, scar of the axillary buttress. Scale bar: 1 cm.

Figure 13. Meiolaniiformes. Left humerus (MPM-PV-22858) in A, dorsal; B, anterior; C, ventral; D, posterior; E, distal views. Abbreviations: cap, capitulum; ecf, ectepicondylar foramen; ect, ectepicondyle; ent entepicondyle; tro, trochlea. Scale bar: 2 cm.

Figure 14. Selected bones of *Isasicursor santacruscesis*. A-B, right maxilla (MPM-PV-22860) in A, medial; and B, lateral views. C-G, proximal end of right ulna (MPM-PV-22861) in C, anterior; D, posterior; E, medial; F, lateral; and G, proximal views. H-L, left metatarsal III (MPM-PV-22862) in H, anterior; I, posterior; J, medial; K, lateral; and L, distal views. Abbreviations: aof; anterorbital fenestra; ap, maxillary ascending process; cp, collateral pit; eg, extensor groove; fg, flexor groove; ig, intercondylar groove; lc, lateral condyle; lr; lateral ridge; lp, lateral process; mc, medial condyle; mp, medial process; mr, medial ridge; ol, olecranon; pr, primary ridge; sr, secondary ridges; tr; teeth root. Scale bar: 2 cm.

Figure 15. Distal end of *Isasicursor santacrucensis* femora showing size variation between the specimens coming from the same spot at the *Isasicursor* II Site.

Figure 16. Indeterminate Enantiornithes. A-K, pedal ungual phalanges (MPM-PV-22867 and MPM-PV-22868 respectively) in A,K, side; B,F, dorsal; C,J, ventral; and D,H, proximal views. Abbreviations: et, extensor tubercle; ft, flexor tubercle; r, ridge; vg, ventral groove. Scale bar: 2 cm.**Figure 17.** Photopanel of the Chorrillo Formation showing the distribution of channelized units (SS and SG; yellow) and non-channelized units (SL, FG and DF; white).

Figure 18. Stratigraphic correlation between Ultima Esperanza, Chile (Manriquez et al., 2019) and south of Lago Argentino, Argentina (this study) showing the fossil content of the main Upper Cretaceous to Paleogene formations of the Magallanes/Austral Basin.

HIGHLIGHTS

*The depositional architectural elements and the paleontological content from the Chorrillo Formation are described.

*The Chorrillo Formation is interpreted as accumulated in a fluvial depositional system dominated by fine-grained deposits.

*The continentalization of the basin provided new ecological niches for plants and vertebrates.

*The fossil vertebrates association matches with the one reported from the Dorotea Formation.

Declaration of interests

☒ The authors declare that they have no known competing financial interests or personal relationships that could have appeared to influence the work reported in this paper.

☐The authors declare the following financial interests/personal relationships which may be considered as potential competing interests: